POLITECNICO DI TORINO

Corso di Laurea Magistrale
in Ingegneria Matematica

Tesi di Laurea Magistrale

Feedback Control Policies and Network Effects in Epidemics Models

Relatori
prof. Fabio Fagnani
prof. Giacomo Como
firma dei relatori

. . . . . .
. . . . . .

Candidato
Martina Alutto

firma del candidato

. . . . . .

Anno Accademico 2020-2021

Abstract

The importance of mathematical models able to predict the dynamic behaviour of an infectious disease has been consolidated in the last year. In this thesis, we examine the SIR compartmental model, both in the scalar and network case, to account for endogenous individuals behaviours and population heterogeneities.

In the first part, after an initial simulation of the classic behaviour, there is a presentation of several modified versions of the model, in which a mitigation term for social interactions is included. This addition, expressed as a function of the fraction of infected, can express either an individual reaction to the presence of the disease or a governments measure, imposed to limit interactions and contain the contagion. Assuming that this function decreases with respect to the number of infected, we demonstrate the existence of a threshold parameter for determining the dynamics, similar to that characteristic of the classic SIR model. The functions considered within the model are different: linear, quadratic, smooth step and smooth. Another analysed case involves piecewise continuous control, in which a lockdown measure is implemented only if the total number of infected reaches a certain threshold level. The long-term behaviour of the system within this strategy consists of the so-called *sliding motion*, which will be presented and studied. Also within the scalar model, a modification will be proposed to take into account a certain delay between the observation of the epidemic and the subsequent responses of individuals or measures adopted by governments, in order to achieve a better description. By merging the concept of piecewise continuous control and delay, there is a continuous transition between the unrestricted model and the model with measures and the *chattering phenomenon* is outlined.

The second part of the thesis focuses on observing the behaviour of the SIR model within a network, in which the population is divided into subpopulations and their interaction is described through a weighted graph. The average behaviour of the model, in which the weights of the average depend on the characteristics of the network, and the behaviour at each component node of the graph are analysed. New results for threshold conditions and stability properties are proposed, focusing in particular on the case of two-nodes networks. In a specific situation of contact between an initially totally healthy node and one with a fraction of infected, we show the occurrence of an atypical phenomenon with respect to the classical SIR theory. We also exhibit how changing the contact between nodes and differentiating the infection rates can affect the dynamics. Then we analysed different versions of lockdown policies within the network model, assuming restrictions between different subpopulations and also within the same subpopulation.

Acknowledgements

Before proceeding with the discussion, I would like to dedicate a few lines to all those who have been close to me on this journey of personal and professional growth.

I would like to express my most sincere thanks and deep gratitude to Professors Fabio Fagnani and Giacomo Como, for their help and support during these months. Although we could not meet in person, they guided me in the writing of this work and conveyed their enthusiasm for the subject matter.

Fundamental throughout my university career has been my family, who have always believed in me and, thanks to their sacrifices, I have been able to face this path with its sweet and tireless support. Thanks also to you, Lollo, for understanding my distance without making me suffer.

Special thanks to Ilaria, my first supporter, my quarantine and travels partner. She listened to me every day, trying to understand as much as possible about this thesis (even if she had to google few terms).

Particular dedication to my friends: first of all, Angi and Franci, my lifelong friends, and then all the others. You have been the fundamental entertainment in these months and years; with you by my side everything has been easier. Thanks also to Cate, Ele e Marghe, my Ligurian friends, for sharing this year with me. Despite the distance and the changes, you have been close to me and I could not ask for better support.

Special mention must also go to my two fellows throughout this experience: your help (material and psychological) has been essential. Federico has been my deskmate, my late-night project partner, and I hope one day to become my work colleague as well. Pier has been my support in these years, a true friend able to cheer me up with a simple dinner out.

Finally, thanks to you Nicolò, you know all my weaknesses and in these months you have tried to erase them and make me feel stronger. I really hope to make you proud of me with this work.

Contents

List of Figures

Chapter 1

Introduction

In the last year, we have witnessed the outbreak of Coronavirus disease, the acute respiratory disease caused by the $2019 - nCoV$ pathogen. This new strain of Coronavirus has emerged in December 2019 in the city of Wuhan (Hubei province, China), and subsequently, with variable disorders and mortality, in various countries around the world. Globally, as of 18 February 2021, there have been 109.594.835 confirmed cases of COVID-19, including 2.424.060 deaths, reported to WHO (*World Health Organization*) [1]. Due to the strong and unexpected pressure on the health system, the worldwide emergency has forced entire nations to impose unprecedented total lockdowns, suspending all but essential activities. Government interventions, to a greater or lesser extent, have been necessary to slow down and limit the propagation of the virus among individuals. This ongoing fight against the spread of the pandemic has revived a keen interest in the analysis of mathematical tools useful in predicting the evolution of the epidemic and in simulations of possible scenarios subjected to different lockdown policies. These instruments may be even more important when the disease has emerged and total prevention is no longer possible. Indeed, if an epidemic outbreak is inevitable, then it is necessary to understand how its severity can be reduced. This renewed focus on epidemiological patterns is also reinforced by the absence or limited availability of an immediate treatment such as a vaccine or a specific cure. In fact, the first difficulty encountered by governments was that of imposing restrictive measures to avoid an exponential increase in the curve of contagions that would result in a unsustainable pressure on the health system. This necessity stems from the absence of a ready remedy against the spread of the virus, such as a vaccine, or even just a specific therapy capable of treating infected patients. The other huge problem associated with this pandemic is the presence of a high percentage of asymptomatic patients, which leads to a dangerous silent spread of the virus. The circulation of a disease among individuals without symptoms is, obviously, more difficult to trace. Unless systematic testing is carried out, the spread of the virus is uncontrolled and also knowledge about the development of the disease asymptomatically remains limited, as do its prevalence and health consequences. Hence the imperative not only to finance scientific research for finding a vaccine, but also to work on intensifying diagnostic testing programmes, in spite of their significant economic cost and the difficulty in planning their optimal administration. Related to this, there is the issue of allocating

resources in a pandemic situation. In the clinical and research setting, resources include test, vaccines but also equipment for therapy such as intensive care beds and ventilators. In economic terms, however, it refers to the funds needed to finance scientific research and, above all, to guarantee isolation and quarantine, with the consequent suspension of certain activities. Within this allocation problem, it is necessary to take into account the differentiation of priorities not only geographically but also in terms of age. There are subpopulations living in sanitary conditions where the virus is more easily transmitted, while at the same time there are age groups that are more vulnerable to infection and have been more affected. This differentiation must be part of the design of the distribution of both health and economic resources available to the population. Nevertheless, a major contribution to the spread of an epidemic is provided by how individuals react to government advice on prevention and various restrictive ordinances. Clearly, when a new disease appears, knowledge and understanding of risk change over time and may be based on different considerations. Therefore information campaigns need to be planned from the early stages of the disease, in order to increase individual awareness of the seriousness and combat misinformation about false cures, anti-vaccine propaganda or conspiracy theories. All the previous considerations underline the absolute necessity, especially at this time, to study mathematical models capable of predicting infections evolution and identifying parameters able to define patterns of behaviour.

The cornerstone in the main epidemiological studies is the classical SIR model of Kermack and McKendrick [2], a deterministic compartmental model that describes a disease propagation among the individuals of a population. The SIR model splits a population into three categories: the *susceptibles*, namely those who have not yet been infected and can catch the disease, the *infected* people, those who are currently carrying the virus and allow the transmission, and finally, the *recovered* people, namely those who have healed from the infection and assumed not susceptible any more. The state is a vector (f_S, f_I, f_R), describing the fraction of the population in the three categories and its time evolution is determined by three coupled ODE's that encorporate the mechanisms of contagion and spontaneous recovery. The transition from one state to the other is expressed through two rates: an infection rate β, which indicates the fraction of susceptibles who become infected in a given time, and a recover rate γ, that determines the transition from infected to recovered. The ratio between the two rates determines the average number of secondary infections generated by a single infective individual in a totally susceptible population and its value is decisive in the dynamics development. The existence of epidemic threshold for the scalar case has been demonstrated and it results that susceptibles must be higher than a critical fraction for an outbreak to occur. Depending on the particular disorder, one might also introduce the state of *exposed*, those who in a latent period have become infected but not yet infectious, or the state of *measles*, which indicates babies born not as susceptible as they are immune to the disease for the first few months of life. Another possibility would be to consider a distinction between *diagnosed* and *undiagnosed* infected individuals, where the former are typically isolated and therefore less likely to spread the infection. Most compartimental models of disease propagation, such as in [3], make the assumption that populations are fully mixed, meaning that an infective individual is equally

likely to spread the infection to any other member of the population. However, this assumption is not realistic, since an infected individual is not as likely to infect everyone else because in real world each individual has contact with only a small fraction of the total population. In order to better describe the pattern of disease spread, several studies have considered topological properties of networks of various types and studied their effects on the epidemic processes taking place on these networks [4]. Through the study of SIR-network models, the topology of the graph has proved to be a determinant feature for the dynamics of the system, as in the paper of Mei et al. [5] where a new threshold condition for epidemic behaviour is proposed in terms of network characteristics, initial conditions and infection parameters. In particular it has been shown how a weighted average of the population of infected people is able to capture all the information on epidemic evolution, where the weights depend on network properties.

The analysis of different models for simulating the spread of an infectious disease and the consequent search for the parameters best able to predict its evolution is now developing in parallel with the study of adeguate lockdown policies for different epidemic scenarios. The main objective in combating an epidemic is, undoubtedly, to control contagion in order to alleviate the health pressure and monitor the development of the infection. Containment of the epidemic curve can be translated into behavioural regulations such as the use of personal protective masks or vaccines and into various lockdown policies, i.e. more or less strong restrictive measures imposed by governments that limit social interactions. An infinite types of emergency restrictions can be studied, involving the whole fraction of infected and susceptible people or a portion of them. In fact, there are certain activities that must be considered as necessary despite the epidemic, such as the opening of grocery stores and pharmacies. A modified version of the SIR that models such policies is presented in Alvarez et al. [6]. From the point of view of finding the optimal policy, one can consider a targeted lockdown for weaker age groups, geographical areas or portions of the population, where the weakness is expressed in terms of greater susceptibility to falling victim to the disease due to age or living conditions. The model developed by Acemoglu et al. [7] introduces a multi-group version of the SIR model to which targeted restrictive policies are applied. Different groups, in this case representing age groups, are treated differently, based on their vulnerability to the epidemic and their economic contribution to society.

The current pandemic has revived interest in the study of optimal control that can minimise both the loss of life and the economic cost of restricting social interactions. Modified versions of the SIR with a control that minimises the outbreak size (or infectious burden) have been studied, taking into account the resource allocation problem mentioned earlier. Hansen and Day in [8] have examined models in which the optimal control was sought under the assumption of limited resources, thus considering the intervention of vaccines and isolation separately. Another category of problems is related to spectral control and optimisation theory [9], where a fixed number of resources must be optimally allocated among a population to best mitigate the effects of an undesirable disease. The modelling hypotheses remain infinite and typically the different considered control leads to completely different solutions. This discussion is part of the study of the resilience property of a graph, i.e. the ability of a system to limit the propagation on a

global scale of any external perturbations or shocks. To analyse the best trade-off between disease victims and economic cost, it is essential to investigate the system's adaptability to changing conditions to forecast the modifications effect on network and to optimize its dynamical behaviour. In this thesis, we will not study optimal control of any kind, limiting the discussion only to analyse and compare the alternative policies. In any case, the application of a control to the model brings to light another issue for policy makers: the start and duration of the interventions. In order to limit the economic impact of the social distancing and quarantine protocols, a time-limited lockdown can be considered. For example, the restrictive measures can be imposed only after a certain level of infection has been reached. In fact, for low values the infection curve can be contained, as can the resulting pressure on the healthcare system; while above a certain threshold, it is necessary to intervene for minimising also the number of victims. The duration of interventions will then be crucial in preventing future outbreaks after the relaxation of the measures.

For infectious diseases, such as the current pandemic, which are mainly transmitted between people through respiratory droplets and contact routes, changes in people's behaviour and, in general, their reaction to the occurrence of the disease must be investigated. Behavioural modifications in response to the outbreak can alter the propagation of a virus, because people aware of their risk can endogenously take measures that modify and reduce their susceptibility. It is therefore important to focus not only on simulating the epidemic outbreak but also the response of individuals to it. Various studies, as [10] and [11], have considered how social and behavioural dynamics could affect the spread of a disease, integrating the concept of knowledge and awareness of the risk of infection into the modelling. In this context, awareness is understood as the possession of information about the epidemic with a consequent willingness to act for reducing own chance of contracting the disease. This is opposed to simply having general knowledge of the disease through media or government programmes without disposition to modify own behaviour. In order to seek a more realistic description of the phenomenon, these aspects must be taken into account as they determine individuals self-regulation on the basis of their own risk and their tendency to obey governments imposed measures as the use of personal protective equipment, compulsory quarantine or the option of vaccination. Therefore, it is worthwhile considering models that incorporate individual responsiveness to external information about a disease. In this thesis, we will only model the response in terms of limiting social interactions with an effect on the contact rate. However, there are several preventive measures, including also pharmaceutival interventions, which have different effects on spread of the disease.

This work presents various extensions of the classical compartimental SIR model. On one hand, we introduce a more complex and realistic interaction function among individuals that encorporates a knowledge of the current fraction of infected and susceptible people. On the other hand, we consider compartimental networked model to simulate heterogeneous behaviours. The outline of this thesis is as follows. In Chapter 2, after an introduction of the classical SIR model, there is a presentation of its different modified versions, in which a mitigation term for social interactions is included. From a modelling point of view, we consider the possible modifications of interactions among individuals

involved in the dynamics either as effect of enforced policies or rather as the effect of increased awareness of the danger due to the disease. We will observe that each of these measures will lead to a containment of contagion but some considerations will need to be made, based on the time at which interactions begin to be limited, the duration of these social restrictions, the rates of infection and recovery from the epidemic. In Chapter 3, initially a result, available in literature, on the threshold parameters and stability conditions in the application of the SIR model in a network is presented. Then the behaviour in different networks and scenarios is analysed. After that, lockdown policies within the network model are examined, assuming restrictions between different subpopulations and also within the same subpopulation.

Chapter 2

Scalar SIR Model

2.1 Original SIR model

In the initial part of the thesis we shall investigate the original SIR model in the scalar case. In this model, we assume that individuals of the population interact with each other uniformly at random, independently from their current state. As a consequence, the growth rate of the fraction of infected individuals is proportional to the product of the fraction of susceptibles and the fraction of infected, multiplied by the so-called *infection rate* $\beta > 0$. Instead the infected individuals heal and move into the recovered state at the *recovery rate* $\gamma > 0$. We will maintain constant the epidemic parameters and use notation $x(t)$, $y(t)$ and $z(t)$ for the fraction of susceptible, infected and recovered respectively. We make the assumption that the total population remains constant over time, i.e. we are not going to consider births or disease deaths. Therefore, we can write the (Susceptible-Infected-Recovered) SIR model without vital dynamics proposed by Kermack and McKendrick [2] as:

$$\begin{cases} \dot{x}(t) = -\beta x(t) y(t) \\ \dot{y}(t) = \beta x(t) y(t) - \gamma y(t) \\ \dot{z}(t) = \gamma y(t) \end{cases} \tag{2.1}$$

where the third equation is redundant.

The susceptibles fraction $x(t)$ is monotonically decreasing and its final number is positive; while the recovered fraction $z(t)$ is monotonically increasing. Regarding the fraction of infected, the determinant of its dynamics is related to the number of susceptibles, still untouched by the disease, and to the epidemic parameters. The infection dies out if enough people are already immune so that an infected individual causes less than a newly infected one. Instead, if an infected individual leads to more than one new infection then the infected fraction is initially increasing until a maximum peak and then becomes decreasing. Let us define the *effective reproduction number* as $R(t) = \beta x(t)/\gamma$, that corresponds to the expected number of individuals that a randomly infected individual can infect during its infection period. We will mainly deal with the value of the reproduction number at the initial instant $R_0 = \beta x(0)/\gamma$. This function of the system variables is fundamental in

predicting what kind of dynamics will develop because it is a parameter able to encapsulate all information about the spread potential of infection. For this reason, the study of this epidemic threshold term will have a key role also in the following parts, when we'll introduce variants to this classical model.

Let us proceed with an initial simulation where we decide to set the infection rate as $\beta = 2$ and recover rate as $\gamma = 0.4$, then we will observe the dynamics of the model in a range period of 30 days, assuming two different set of initial conditions. In the first case we've set $(x(0), y(0), z(0)) = (0.19, 0.81, 0)$ so that the initial effective reproduction number is less than 1. In the second case $(x(0), y(0), z(0)) = (0.95, 0.05, 0)$ and this implies $R_0 > 1$. The experimental set-ups used does not include any initial fraction of recovered, meaning that the infection has just emerged in the population and/or no data on cured people have yet been collected. This will be a constant assumption throughout the discussion unless otherwise specified.

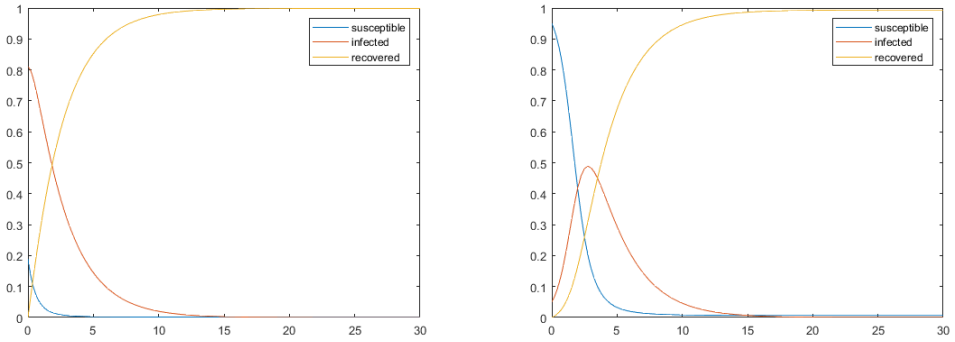

(a) (b)

Figure 2.1: Scalar SIR model simulation. In (a), the initial effective reproduction number is below the threshold value of the epidemic and we can see a monotonically decreasing trend of the infected curve. While in (b) the infected curve shows an initial exponential growth, it reaches the maximum and then it monotonically decreases to 0.

The simulations shown in the Figure 2.1 confirm the behaviour of the curve of infected explained before. This is clearly dependent on the initial effective reproduction number R_0. However, we observe that the susceptible and recovered curves has the same general performance in both simulation cases.

Once we have understood the trend of the original model, we can use these results to consider some modifications. Observing the previous simulations, in particular where there is an initial exponential growth of the $y(t)$ curve, it proves to be crucial to integrate in the model a mitigation function of the interactions for a contagion limitation.

2.2 A controlled SIR model

As we mentioned in the introduction, several modified versions of the SIR model have been studied over the last years. The modification with respect to the classical model consists in a term of reduction of social interactions between individuals. This control is introduced with the main aim of containing the infection curve and thus alleviating the pressure on the healthcare system. Often this objective must also take into account a minimisation of the economic costs arising from the restrictive policies adopted. In this section we will not discuss about optimal control but we will analyse the behaviour of modified SIR models and then compare different hypotheses of social distancing measures. We will therefore consider several mitigation terms, that can be interpreted as a individual behavioural response following the emergence of the infection or as a regulation imposed by governments. In both assumptions, these additions will affect the contact rate between infected and susceptibles and, then, the infection transmission.

Therefore let us introduce a control $h : [0,1]^2 \mapsto \mathbb{R}^+$, that is a function of the number of susceptibles and infected and expresses a lockdown effect in which contacts between individuals are limited. This function can initially be interpreted either as a lockdown policy imposed by governments or as a limitation of interactions that occurred as an individual reaction to the epidemic. We can imagine that each individual, depending on his perception of the risk, is willing to restrict social activities regardless of government orders. In our simulations we assume this kind of individual, who has a rational behavioural reaction of restricting interactions that is directly proportional to the current number of infected and susceptibles. Therefore, we will consider the modified version of the SIR model below.

$$\begin{cases} \dot{x}(t) = -x(t)y(t)h(x(t), y(t)) \\ \dot{y}(t) = x(t)y(t)h(x(t), y(t)) - \gamma y(t) \\ \dot{z}(t) = \gamma y(t) \end{cases} \tag{2.2}$$

Let us now examine its dynamical behaviour as a generalization of the classical SIR model.

Theorem 2.1. *Consider the model (2.2) with a continuous control $h(x, y) : [0,1]^2 \mapsto \mathbb{R}^+$, $h \in C^1$ that is increasing with respect to x, i.e. $\partial h/\partial x > 0$. Suppose an initial condition such that $x(0) + y(0) + z(0) = 1$, $x(0)$, $y(0) > 0$ and $z(0) \geq 0$. Then the following statements hold:*

1. *$x(t) > 0, y(t) > 0, z(t) \geq 0$ and $x(t) + y(t) + z(t) = 1$ for all $t \geq 0$;*
2. *The susceptibles function $t \mapsto x(t)$ is monotonically decreasing and the recovered function $t \mapsto z(t)$ is monotonically increasing;*
3. *Define the set*
$$\Omega = \{(x, y) \in [0,1]^2 : xyh(x, y) - \gamma y < 0\} \tag{2.3}$$
then Ω is an invariant set for the dynamics,
4. *For any initial condition $(x_0, y_0) \notin \Omega$, there exists an instant $t^* > 0$:*
$$(x(t), y(t)) \in \Omega \quad \forall t > t^* \tag{2.4}$$
$$(x(t), y(t)) \notin \Omega \quad \forall t < t^* \tag{2.5}$$

Proof. Integrating the first two equations in (2.2) yields

$$x(t) = x(0)e^{-\int_0^t y(\tau)h(x(\tau),y(\tau))d\tau} > 0 \quad \forall t \geq 0 \tag{2.6}$$

$$y(t) = y(0)e^{\int_0^t (x(\tau)h(x(\tau),y(\tau))-\gamma)d\tau} > 0 \quad \forall t \geq 0 \tag{2.7}$$

This implies that $x(t) > 0$, $y(t) > 0$ for all $t \geq 0$. The third equation in (2.2) instead yields

$$z(t) = z(0) + \int_0^t \gamma y(\tau)d\tau \geq 0 \quad \forall t \geq 0 \tag{2.8}$$

Since $y(t) > 0$, we also have that $z(t) > 0$ for all $t \geq 0$. To complete 1), we can observe that

$$\dot{x}(t) + \dot{y}(t) + \dot{z}(t) = 0 \quad \Rightarrow \quad x(t) + y(t) + z(t) = 1 \quad \forall t \geq 0 \tag{2.9}$$

since $x(0) + y(0) + z(0) = 1$.

Concerning 2), having shown the positivity of the three system variables, it must be $-x(t)y(t)h(x(t), y(t)) < 0$ and, analogously, $\gamma y(t) > 0$, $\forall t \geq 0$. We can therefore state that $x(t)$ is monotonically decreasing, while $z(t)$ is monotonically increasing.

Regarding statement 3), consider an initial condition $(x_0, y_0) \in \Omega$ and let $(x(t), y(t))$ be the corresponding solution. We want to proof that $(x(t), y(t)) \in \Omega \quad \forall t$, i.e. if the system has initial conditions that make fraction of infected decreasing, then this fraction will remain decreasing $\forall t \geq 0$. If this does not hold true, then it must exist an instant $t^* > 0$ such that

$$(x(t^*), y(t^*)) \in \delta\Omega = \{(x, y) \in [0,1]^2 : xyh(x, y) - \gamma y = 0\} \tag{2.10}$$

and $(x(t), y(t)) \in \Omega \quad \forall t < t^*$. Let us define

$$V(t) = xyh(x, y) - \gamma y \tag{2.11}$$

and consider its first derivative with respect to time t.

$$V'(t) = \dot{x}yh + x\dot{y}h + xy\left(\frac{\partial h}{\partial x}\dot{x} + \frac{\partial h}{\partial y}\dot{y}\right) - \gamma\dot{y} \tag{2.12}$$

Notice that, necessarily, $y(t^*) > 0$ and $\dot{y}(t^*) = 0$ and remember $\partial h/\partial x > 0$. Hence, $V'(t^*) < 0$ and, by continuity, we can state that $V'(t) < 0$ in a neighborhood $(t^* - \epsilon, t^*]$. Since V is decreasing and, by construction, $V(t) < 0$ for $t < t^*$, it is not possible that $V(t^*) = 0$ and this proves the statement 3).

For statement 4), having shown the previous point, we only have to prove that exists an instant t^* such that $(x(t^*), y(t^*)) \in \Omega$. If this was not the case, then it would be $\dot{y}(t) > 0 \, \forall t$ and $y(t)$ would not tend to 0. Therefore $z(t)$ would blow up which is impossible for the first statement. □

Remark 1. *We can recover the known results for the classical SIR model setting $h(x, y) = \beta$ constant $\forall (x, y) \in [0,1]^2$. In fact, $(x_0, y_0) \in \Omega$ means $\beta x_0/\gamma < 1$. In this case, we can obtain the expression of the maximum fraction of infected as*

$$y_{max} = x(0) + y(0) - \frac{\gamma}{\beta}\left(\ln(x(0)) + 1 - \ln(\frac{\gamma}{\beta})\right)$$

Remark 2. *The function $R^m(t)$, defined as $\beta x(t)h(x(t), y(t))/\gamma$, plays a key role of a novel effective reproduction number, in which the modification to interactions, included in the model, is taken into account.*

In the remaining part of this chapter, we will consider a mitigation function of social interactions that depends only on the fraction of infected y. This term will always be assumed to be decreasing with respect to the number of infected, as we recall that it corresponds to a limitation of contacts as an individual response to the epidemic or a restrictive measure imposed by governments. In particular, we will consider a model of the type

$$\begin{cases} \dot{x}(t) = -\beta x(t)y(t)f^2(y(t)) \\ \dot{y}(t) = \beta x(t)y(t)f^2(y(t)) - \gamma y(t) \\ \dot{z}(t) = \gamma y(t) \end{cases} \tag{2.13}$$

where $f(y)$ is a function of the number of infected and indicates a mitigation of contacts between the susceptible and infected. It is considered quadratic to take into account that a more densely occupied environment leads to more contacts in strict proportion to density. For our simulation purposes, we will always consider a decreasing function in $y(t)$ that maps from [0,1] to [0,1]. For example, we would suppose $f(y) = 1 - y$ or $f(y) = (1 - y)^2$, or in general some decreasing smooth function.

2.2.1 Simulations with different continuous control actions

Having shown the existence of an epidemic threshold value also for this modified version of the SIR model, we can now proceed with some simulations. Let us suppose a *linear* $f(y) = 1-y$, and a *quadratic* $f(y) = (1-y)^2$ mitigation function, assuming again infection rate as $\beta = 2$ and recover rate as $\gamma = 0.4$.

In the following figures, there are the simulations of the original SIR model and the two modified versions with two different initial conditions. In the first set, the initial conditions used are $(x(0), y(0), z(0)) = (0.19, 0.81, 0)$, such that the infected curve is expected to be monotonically exponentially decreasing to 0. In the second set of plots, we use instead $(x(0), y(0), z(0)) = (0.95, 0.05, 0)$, in order to have a unimodal behaviour for the curve of infected. As the exponent considered in the social limitation function increases, a delay in the attainment of the maximum and a decrease of such value can be noticed.

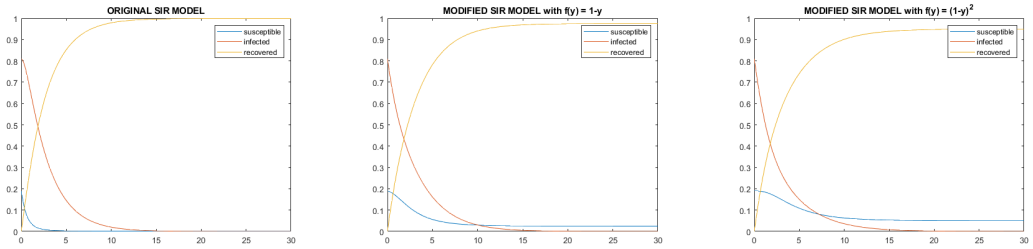

(a) (b) (c)

Figure 2.2: Simulation of the SIR model with the classical and new reproduction numbers below 1. The first figure on the left is the original model, while the other two figures are the simulations of the modified SIR model with linear and quadratic interaction terms.

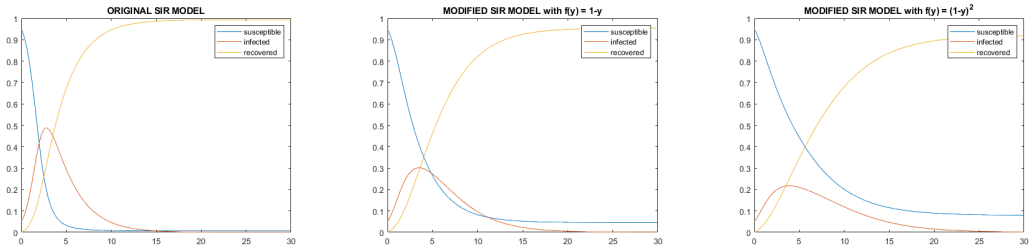

(a) (b) (c)

Figure 2.3: Simulation of the SIR model with the classical and new reproduction numbers above 1. The first figure on the left is the original model, while the other two figures are the simulations of the modified SIR model with linear and quadratic interaction terms.

As far as the first part of the simulations is concerned, the limitation of the interactions, added to the original model, modifies the monotonically decreasing trend of the infected curve, which does not undergo a rapid decrease but is more flattened. In fact, it results in an increasingly lower fraction of final recovered as the exponent α increases. In the second part of the simulations, on the contrary, we observe an attenuation of the peak of infection and a delay in reaching it. The effect of pattern modification also occurs in the final fraction of susceptibles, which increases as the strength of the restriction intensifies.

After studying the behaviour of the SIR model with the introduction of a function as $f(y) = (1-y)^\alpha$ with $\alpha > 0$ that aims to mitigate social interactions between individuals with a dependence on the fraction of infected, we can suppose another kind of function. As a first assumption, we can consider a *smooth step functio*n, i.e. a *S-shaped* sigmoid curve with the following definition

$$f(y) = \begin{cases} 1 & if \quad 0 \leq y \leq y_1 \\ ay^3 + by^2 + cy + d & if \quad y_1 \leq y \leq y_2 \\ 0 & if \quad y_2 \leq y \leq 1 \end{cases}$$

where y_1, y_2 are two endpoints and a, b, c, d are coefficients that we are going to determine in order to obtain a functional tool in this problem. We decide to set $y_1 = 0$ to start immediately with the containment of infected propagation and $y_2 = 0.7$ as there would be a too high fraction of infected and this can justify a total lockdown. By imposing the condition of continuity in the two endpoints and the condition of the zero first derivative in these points, we get the following values: $a = 5.83$, $b = -6.12$, $c = 0$, $d = 1$. Let us compare the different types of functions considered within the model in the following figure.

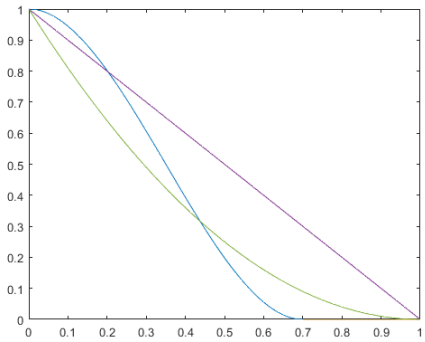

Figure 2.4: Graph of the three functions used as lockdown measurements in the range [0,1]. The violet line is the function $f(y) = 1 - y$, the green curve is $f(y) = (1 - y)^2$, while the blue one is the smooth step function described above.

Observing the graph, we find an interesting trend of the function based on our aim in this section: in fact, initially the smooth step function is equal to 1, then for low infection values, it remains above the straight line so it results in a milder limitation of interactions. After that, the function is located between the straight line and the parabola, leading to a more intelligent and strict lockdown at higher infection values, up to the total shutdown of interactions for infection values above 0.7.

In this chapter, our aim is not to determine the "best control" of infection in terms of minimising contagion and economic cost of limiting social activities. We only intend to analyse the effect on the overall dynamics of including different functions of the infected in the classical model. Therefore, we will only insert this function into the modified SIR model and observe how the dynamics have changed with respect to the classical and other modified cases.

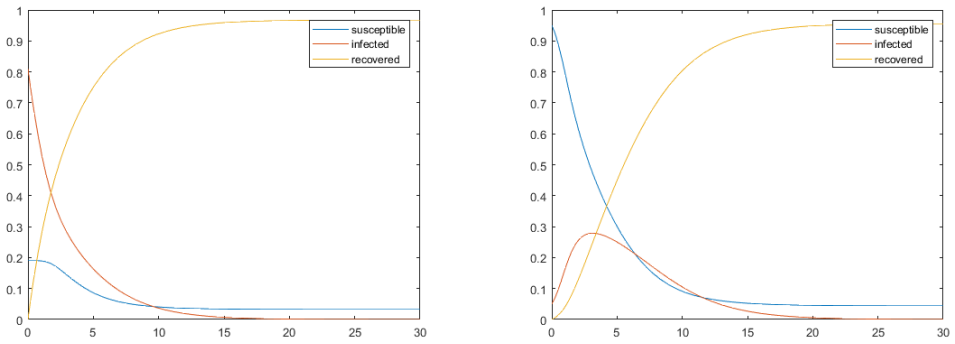

(a) (b)

Figure 2.5: Simulation of the modified SIR model with smooth step mitigation term. On the left, the new reproduction number is below 1, while in the right figure it is above 1.

We would like to focus our analysis on the case in which the curve of the infected has a unimodal behavior. We can make a comparison between the dynamics of the original SIR and those achieved by inserting some mitigation functions in the model. With the particular data set used, the SIR model has an infection peak of about 0.49. This peak is reduced to 0.30 when $f(y) = 1 - y$, and further reduced to 0.22 when $f(y) = (1 - y)^2$, instead when $f(y)$ is the smooth step function it's about 0.28. This results in a general attenuation of the curve and, consequently, in an increase of the final fraction of susceptible individuals. The portion of individuals remaining susceptibles, and therefore not affected by the epidemic, are 0.007 in the original SIR scenario, 0.045 with the linear function, 0.08 with the parabola, 0.044 with the smooth step function. We can therefore observe that the quadratic dependence of the infected variable remains the measure leading to the lowest peak of infection and to the highest final fraction of susceptibles with the particular set of values used.

A further hypothesis may be to consider another *smooth function* as a mitigation of social interactions to be included in the modified SIR model that presents a similar trend to the previous one. For example, we can assume that

$$f(y) = (1 - y^2)^\alpha$$

with $\alpha > 0$, that determines the strength of the restriction. In order to obtain a more severe limitation than the smooth step function, we choose $\alpha = 7$. Let us first observe the trend of this function for $y \in [0,1]$ with respect to the other mitigation functions used previously.

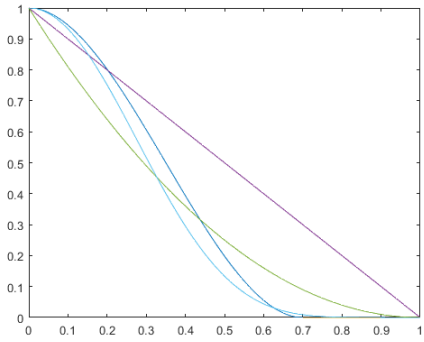

Figure 2.6: The four functions used as lockdown measures, in the range [0,1]. The violet line is the function $f(y) = 1 - y$, the green line is $f(y) = (1 - y)^2$, the blue one is the smooth step function and the light blue is the smooth function.

In the following figure, the simulation of the modified model with the insertion of the smooth function is shown. It can be argued that the increase in the exponent α considered would lead to a greater lockdown effect resulting in a more restrictive shutdown of social and commercial activities of the population, but this is not the subject of our analysis.

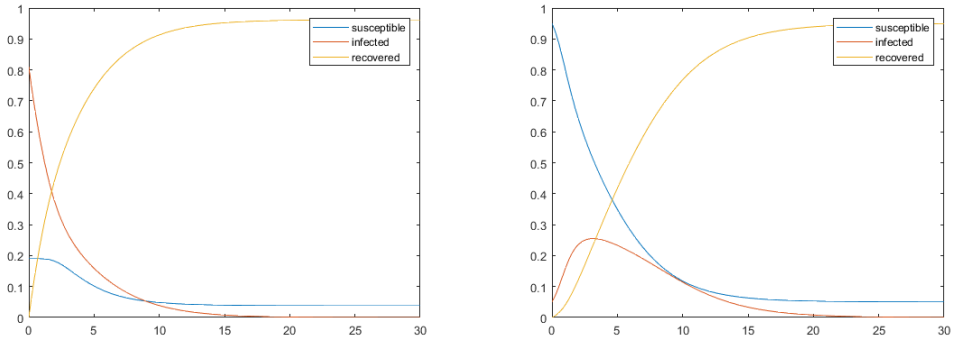

(a) (b)

Figure 2.7: Simulation of the modified SIR model with smooth mitigation term. On the left, the new basic reproduction number is below 1, while the right one is above 1.

In case the infected curve has a peak, it is worth 0.25, so a higher attenuation than in the case of the straight line or smooth step function, leading to a final susceptible fraction of 0.05. The use of the quadratic control action in this simulation set-up for the scalar model is confirmed as the best way to guarantee a greater final portion of susceptibles, who remained untouched by the epidemic.

2.2.2 Modified SIR model with measures relaxed after a certain period of time

We have previously assumed that the interval time of implementation of restrictive measures coincides with the entire course of the disease. However, it is not realistic to assume, for example, that the nature of the individual's reaction will be the same throughout the period of the emergency or, above all, that the measures imposed by the governments will remain in place unchanged until the disease has completely disappeared. For this reason, an important question is whether to relax after a certain period of time the restrictive measures or to keep them active throughout the epidemic as previously simulated. The debate also concerns the modality, i.e. whether to alleviate the measures partially or totally, and when to relax them.

We will see that this decision will have to be significantly linked to the verification of the achievement of the *herd immunity level*. This term indicates the level of the population immunity at which the spread of the disease will decline and stop even after the preventive measures have been relaxed. Within the SIR model studied, we will consider as immune the infected individuals, who cannot take the virus because they have already been infected and the recovered, that are healed after the infection and now immune. It is therefore crucial to consider how many people have been affected by the disease and, consequently, the fraction of remaining susceptibles before deciding to relax restrictive measures. If *herd immunity level* is not achieved, then a second wave of infection may start once restrictions are lifted. We will consider only the case where the measures are totally eliminated after a certain period. The time instant t^* when these measures are slowed down, must be characterized by an effective reproduction number of the classical SIR $R(t^*)$ less than 1 in order to ensure a natural decline of epidemic contagion. It must therefore result that

$$R(t^*) = \frac{\beta}{\gamma} x(t^*) < 1 \quad \Leftrightarrow \quad x(t^*) < \frac{\gamma}{\beta}$$

so we can define the herd immunity level as $h = 1 - \gamma/\beta$.

Let us now observe the evolution of the curve of the infected in cases where preventive measures (in the form of $f(y(t)) = 1 - y(t)$) are maintained for a certain period of time from the initial instant of simulation. In the figure below, the lockdown policy is completely removed after 3,4,5,6 days. The initial conditions used are $(x(0), y(0), z(0)) = (0.95, 0.05, 0)$ with $\beta = 2$ and $\gamma = 0.4$ as system parameters. We can note that

$$R_0^m = \frac{\beta}{\gamma} x(0) f(y(0))^2 \simeq 4.3 > 1$$

Therefore, this experimental set-up is such as to guarantee for the modified SIR model a unimodal behaviour of the infected curve according to what has been demonstrated in the Theorem 2.1.

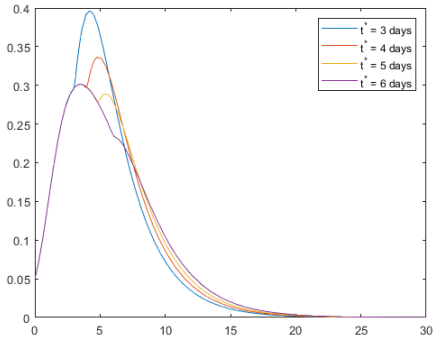

Figure 2.8: Evolution of the infected curve $y(t)$ where at time $t^* = 3,4,5,6$ days the restrictive measures are relaxed.

We can observe that the measures relaxation after 3,4 and 5 days leads to the occurrence of a second peak of infection after few days. This phenomenon is caused by the fact that the level of herd immunity has not yet been reached, so the number of susceptible individuals is still too high to avoid the epidemic outbreak. The second wave of infection does not occur if the measures are lifted after 6 days, so this means that between the fifth and sixth day the population reaches the level of immunity that causes the decline of the infected curve regardless of the measures taken.

Let us now summarise in a corollary some considerations arising from the theorems on the dynamics of the classical and modified SIR model.

Corollary 2.1.1. *Consider the modified version of the SIR model (2.2) with a control measure $f : [0,1] \to [0,1]$, function of the infected variable y. Assume f is not increasing in its domain for an initial time interval $[0, t^*]$, after which this restrictive measure is lifted and the model is returned to its original SIR. Let us suppose as initial conditions $x(0) + y(0) + z(0) = 1$, with $x(0), y(0) > 0$ and $z(0) \geq 0$. Then the following statements hold:*

1. *For $t \in [0, t^*]$ the restrictive measure is active and depending on the initial reproduction number of the modified SIR model*

$$R_0^m = \frac{\beta}{\gamma} x(0) f(y(0))^2$$

   the resulting infected function $t \mapsto y(t)$ will either be monotonically and exponentially decreasing ($R_0^m < 1$) or show an unimodal behaviour ($R_0^m > 1$).

2. *After that time interval, the lockdown measures are released and the model corresponds to the original SIR. The infected trajectory behaves as follows:*

   a) if $\beta x(t^*)/\gamma < 1$, then $t \mapsto y(t)$ exponentially decreases to 0 as $t \to \infty$.

   b) if $\beta x(t^*)/\gamma > 1$, then $t \mapsto y(t)$ presents a second peak and then decreases to 0.

The previous corollary underlines the need to introduce and maintain a control at least until the level of herd immunity is reached, in order to ensure a unimodal behaviour for the curve of the infected as it occurs for the classical SIR model. The appearance of a second peak of infection and outbreak of the epidemic could happen if the fraction of susceptibles, left untouched by the disease, is still too high when the measures are removed.

2.3 The case of a discontinuous control

The model considered so far assumes the control action to be continuous in the fraction of infected individuals. If this is suitable in modelling self-reactions to an epidemic spreading, it is restrictive when modelling lockdown policies. Previously, we have assumed that the imposed measures take effect from the very first time instant of model simulation and they could be at most released after a certain period of time. However, especially in the most recent phase of the COVID-19 emergency, governments have only applied lockdown policies when the number of infected people, relative to the amount of diagnostic tests performed, exceeds a critical percentage. In this section we will consider a system in which control is implemented only when the total number of infected reaches a certain threshold level, that is considered dangerous due to its consequences on the health and economic system. It is necessary to analyse more accurately this version of model, in which we decide to introduce a piecewise continuous control function that regulates the strategy of disease management, based on the number of infected people.

We will carry out a similar analysis to that conducted by Xiao et al. in [12]. The proposed model extends the original SIR model, adding a mitigation rate of social interactions activated only once the number of infected individuals exceeds a threshold level. The long-term behaviour of the system within this strategy could consist of the so-called sliding motion, i.e. a very rapid transition between application and interruption of the control action. Sliding mode control is a non-linear control method that modifies the dynamics of a nonlinear system by applying a discontinous control signal [13]. The control structure is designed so that the system remains confined to the adjacent region with the different control structures (called the *sliding mode region* or *domain*) and is forced to slide along it. In these systems, the right-hand side (the vector field) varies discontinuously as solution trajectories reach the sliding surface. The aim of this section is therefore to formulate a new mathematical model subject to the threshold policy and to study a system of Filippov [14]. Let us begin with a brief review of the approach as in [15], proposed by Filippov, to define the solution on the sliding surface.

Filippov convex method. Consider the discontinuous differential system

$$x'(t) = f(x(t)) = \begin{cases} f_1(x(t)), & h(x) < 0 \\ f_2(x(t)), & h(x) > 0 \end{cases} \qquad x(0) = x_0 \in \mathbb{R}^n \tag{2.14}$$

Suppose the state space $\mathbb{R}^n$ is split into two subspaces Σ_1 and Σ_2 by a surface Σ such that $\mathbb{R}^n = \Sigma_1 \cup \Sigma \cup \Sigma_2$. The surface Σ is defined by the scalar function $h : \mathbb{R}^n \to \mathbb{R}$, so that

$$\Sigma_1 = \{x \in \mathbb{R}^n | h(x) < 0\}, \tag{2.15}$$

$$\Sigma_2 = \{x \in \mathbb{R}^n | h(x) > 0\}, \tag{2.16}$$

$$\Sigma = \{x \in \mathbb{R}^n | h(x) = 0\} \tag{2.17}$$

Assume also that the gradient $\triangle h(x) \neq 0$ at all $x \in \Sigma$. Define

$$n(x) = \frac{\triangle h(x)}{\| \triangle h(x) \|} \tag{2.18}$$

for the unit normal to Σ.
In (2.14), the right-hand side $f(x)$ can be assumed to be smooth on Σ_1 and Σ_2 separately. Let us assume that f_1 is C^2 on $\Sigma \cup \Sigma_1$ and f_2 is C^2 on $\Sigma \cup \Sigma_2$. If $x \in \Sigma$ and

$$n^T(x) f_1(x) > 0 \quad and \quad n^T(x) f_2(x) < 0 \tag{2.19}$$

then the one has so-called sliding motion on Σ. Filippov defines the sliding motion as the solution of the differential system

$$x'(t) \in F(x(t)) = \begin{cases} f_1(x(t)), & h(x) < 0 \\ f_F(x(t)), & h(x) = 0 \\ f_2(x(t)), & h(x) > 0 \end{cases} \tag{2.20}$$

where the vector field on the surface is taken to be in the convex hull $co(f_1, f_2)$ of f_1, f_2, that is

$$co(f_1, f_2) = \{f_F \in \mathbb{R}^n : f_F = \alpha f_2 + (1 - \alpha) f_1, \, \alpha \in [0,1]\} \tag{2.21}$$

and $\alpha(x)$ is chosen so that $n^T(x) f_F(x) = 0$. The extension of a discontinuous system into a convex differential inclusion (2.20) is known as *Filippov convex method*. Existence of solutions of (2.14) can be guaranteed with the notion of upper semi-continuity of set-valued functions.

Definition 1. *(Solution in the sense of Filippov). An absolutely continuous function $x : [0, \tau) \mapsto \mathbb{R}^n$ is said to be a solution of (2.14) in the sense of Filippov, if for almost all $t \in [0, \tau)$ it holds that*

$$x'(t) \in F(x(t)),$$

where $F(x(t))$ is the closed convex hull in (2.21).

SIR sliding mode.

After this brief theoretical overview of the problem, we proceed to study the following modified SIR model.

$$\begin{cases} \dot{x}(t) = -\beta x(t) y(t) f^2(y(t)) \\ \dot{y}(t) = \beta x(t) y(t) f(y(t)) - \gamma y(t) \\ \dot{z}(t) = \gamma y(t) \end{cases} \tag{2.22}$$

where

$$f(y) = \begin{cases} 1 & if \quad h(y) = y - k < 0 \\ g(y) & if \quad h(y) = y - k > 0 \end{cases} \tag{2.23}$$

where $g : [0,1] \to [0,1]$ defines a control function that is active only when the fraction of infected y is above a predefined threshold level $k \in [0,1]$.

Considering only the first two equations of the model, we can call the structure without intervention ($f(y) = 1$) as *free system* and the structure with intervention ($f(y) = g(y)$) as *controlled system*. Obviously, the first case is the classical SIR model, while the second is the modified SIR model with a mitigation function. The sliding mode along the threshold level k may ensue in case, in its proximity, the vector fields of the two structures are directed towards each other. In both cases, we have already presented and studied the dynamics, now we can proceed to analyse their combination.

According to the Filippov convex method, we can define

$$f_1(x,y) = (-\beta xy, \beta xy - \gamma y)^T \tag{2.24}$$

$$f_2(x,y) = \left(-\beta xyg^2(y), \beta xyg^2(y) - \gamma y\right)^T \tag{2.25}$$

then the system (2.22) with (2.23) can be rewritten as the following Filippov system by setting $Z = (x,y)$

$$\frac{dZ}{dt} = \begin{cases} f_1(x,y), & (x,y) \in \Sigma_1 \\ f_2(x,y), & (x,y) \in \Sigma_2 \end{cases} \tag{2.26}$$

where

$$\Sigma_1 = \{(x,y) \in \mathbb{R}^2 : y < k\}, \quad \Sigma_2 = \{(x,y) \in \mathbb{R}^2 : y > k\} \tag{2.27}$$

Furthermore, we can define the manifold Σ as

$$\Sigma = \{(x,y) \in \mathbb{R}^2 : y = k\} \tag{2.28}$$

which is a discontinuity surface between the two different structures of the system. A sliding mode exists if there are regions in the vicinity of manifold Σ where vector fields for the two different structures of the system are directed toward each other.
Precisely, if for $(x,y) \in \Sigma$, we have

$$n^T(x,y)f_1(x,y) > 0 \quad \textit{and} \quad n^T(x,y)f_2(x,y) < 0 \tag{2.29}$$

then we have the so-called sliding mode through (x,y). We can solve the previous inequalities with respect to x and we find that

$$\frac{\gamma}{\beta} \leq x \leq \frac{\gamma}{\beta g^2(k)} \tag{2.30}$$

The sliding mode region becomes

$$\Omega = \{(x,y) \in \mathbb{R}^2 : \frac{\gamma}{\beta} \leq x \leq \frac{\gamma}{\beta g^2(k)},\ y = k\} \tag{2.31}$$

We can prooced with algebraic manipulations in order to show and describe sliding mode dynamics along the manifold. We can eliminate the control $f(y)$ and note that $\dot{h} = \dot{y} = \beta xyf^2(y) - \gamma y$. If $\dot{h} = 0$, then

$$f^2(y) = \frac{\gamma}{\beta x}$$

Substituting the control $f^2(y)$ given above and $y = k$ into the first equation of the model gives the system dynamics on the switching line

$$\dot{x}(t) = -\gamma k$$

which means that the sliding mode has no equilibrium and when trajectories hit the sliding mode region, the state vector starts to move along the manifold, converging to the end point of this domain.

Constant control. As first case, we consider a piecewise constant control. Let us analyse the model (2.22) with

$$f(y) = \begin{cases} 1 & if \quad h(y) = y - k < 0 \\ \delta & if \quad h(y) = y - k > 0 \end{cases} \tag{2.32}$$

where $\delta \in [0,1)$ represents a constant limitation of social interactions when the infection is too high. Before proceeding with the analysis of the sliding mode, let us analyse the system's vector field pattern. Assume initially that the constant control is such that $\frac{\gamma}{\delta\beta} < 1$, consequently the sliding manifold will become

$$\Omega = \left\{ (x,y) \in \mathbb{R}^2 : \quad \frac{\gamma}{\beta} \leq x \leq 1, \quad y = k \right\} \tag{2.33}$$

All trajectories, with a classical reproduction number R_0 above 1, will eventually hit the manifold. If, on the other hand, $\frac{\gamma}{\delta\beta} > 1$, then the sliding mode region is defined as

$$\Omega = \left\{ (x,y) \in \mathbb{R}^2 : \quad \frac{\gamma}{\beta} \leq x \leq \frac{\gamma}{\delta\beta}, \quad y = k \right\} \tag{2.34}$$

and depending on the initial conditions with respect to the threshold value chosen, sliding mode may or may not occur.

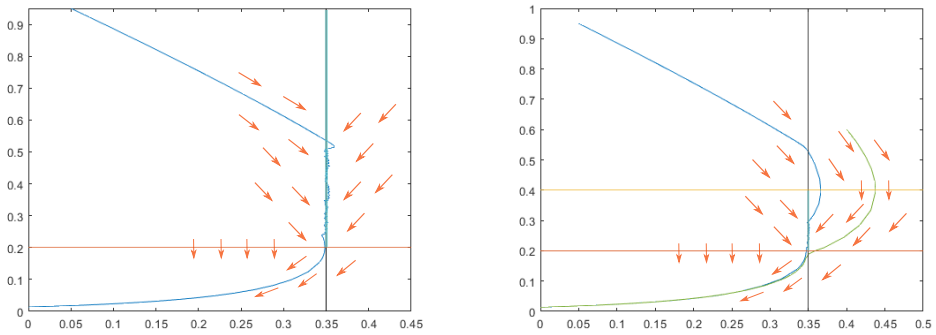

(a) (b)

Figure 2.9: Vector field pattern for a system with a piecewise constant control function. On the left (a), $\frac{\gamma}{\delta\beta} < 1$, the *blue* curve is a solution, while the *red* line defines the lower boundary of sliding mode region (underlined in blue). On the right (b), $\frac{\gamma}{\delta\beta} > 1$, the *blue* and *green* curves are possible solutions for different initial conditions, with the *red* and *yellow* lines define the sliding mode region. In both figures, the *black* line is $y = k$.

In the previous figure we can observe the system's vector field pattern in the phase plan with infected on the orizontal axis and susceptibles on vertical axis. In the first case, the sliding mode occurs in any scenario in which the initial reproduction number of the classical SIR model is greater than 1. In the second case, however, we note that depending on the initial conditions, there may be trajectories that never hit the sliding mode region and others that, after an initial outbreak in the controlled model, enter that region.

We can now examine the sliding mode existence for this model. Let us first remember from the classical SIR theory

$$y_{max} = x(0) + y(0) - \frac{\gamma}{\beta}\left(\ln(x(0)) + 1 - \ln\left(\frac{\gamma}{\beta}\right)\right) \tag{2.35}$$

as the maximum fraction of infected of the classical SIR given $(x(0), y(0), z(0))$ as initial condition.

Proposition 2.2. *Consider the modified SIR model (2.22) with a piecewise constant control (2.32) and initial condition $(x_0, y_0, 0)$. Let us define $k \in [0,1]$ as the threshold level of infection, $R_0 = \beta x_0/\gamma$ as the classical SIR reproduction number, while $R_0^m = \delta\beta x_0/\gamma$ as the controlled SIR reproduction number. If*

$$\frac{\gamma}{\beta}\ln\left(\frac{1}{R_0^m}\right) + 1 - \frac{\gamma}{\delta\beta} + \leq k \leq \frac{\gamma}{\beta}\ln\left(\frac{1}{R_0}\right) + 1 - \frac{\gamma}{\beta} \tag{2.36}$$

then the sliding motion along the manifold Σ exists and the solution (x, y) will hit this surface directly without infected exceeding threshold level k.

Proof. To ensure that the solution hits the sliding mode region (2.34), we must surely have

$$k < y_{max} = \frac{\gamma}{\beta}\ln\left(\frac{1}{R_0}\right) + 1 - \frac{\gamma}{\beta} \tag{2.37}$$

since there is no initial fraction of recovered.

Let us consider the case in which the solution runs entirely through the manifold. Recall from the classical SIR theory, the relation that links the fraction of infected y to the fraction of susceptible x at each instant t of the solution.

$$x(t) - \frac{\gamma}{\beta}\ln(x(t)) = x_0 + y_0 - y(t) - \frac{\gamma}{\beta}\ln(x_0) \tag{2.38}$$

We impose that the solution passes through point $(k, \frac{\gamma}{\delta\beta})$ of the phase plan, i.e. the starting point of the sliding mode region. We obtain that

$$\frac{\gamma}{\delta\beta} - \frac{\gamma}{\beta}\ln\left(\frac{\gamma}{\delta\beta}\right) = x_0 + y_0 - k - \frac{\gamma}{\beta}\ln(x_0) = 1 - k - \frac{\gamma}{\beta}\ln(x_0) \tag{2.39}$$

The threshold level k, for which the sliding mode region is entirely run, is

$$k = 1 - \frac{\gamma}{\delta\beta} + \frac{\gamma}{\beta}\ln\left(\frac{\gamma}{\delta\beta x_0}\right) = 1 - \frac{\gamma}{\delta\beta} + \frac{\gamma}{\beta}\ln\left(\frac{1}{R_0^m}\right) \tag{2.40}$$

Therefore, if k is greater than this value, then the sliding mode occurs along the manifold Ω and it hits this region with a fraction of susceptibles less than or equal to $\gamma/(\delta\beta)$. This guarantees the existence of the sliding motion since the two vector fields are directed toward each other. □

Remark 3. *If $k > y_{max}$, then the sliding motion along the manifold Σ does not exist. If the classical SIR infected curve grows up to y_{max} without control, then the modified SIR model is never activated and the model (2.22) coincides with the classical SIR.*

Remark 4. *If $k < 1 - \gamma/(\delta\beta) + \gamma/\beta \ln(1/R_0^m)$, then there is an outbreak of the epidemic even in the controlled system because the solution hits the manifold with a number of susceptibles greater than $\gamma/(\delta\beta)$. This behaviour may causes the disappearance of the sliding mode. If the curve of the infected reaches the switching surface for the second time with a number of susceptibles less than γ/β, then the sliding mode surely does not exist because the solution does not hit Ω.*

As previously said, $k = 1 - \gamma/(\delta\beta) + \gamma/\beta \ln(1/R_0^m)$ is the threshold level for which the solution hits the sliding mode region precisely in its initial point and it runs entirely through it. For smaller values, there will be trajectories that cause an outbreak in the sense that the number of infecteds initially exceeds k.

Let us consider the model (2.22) with a piecewise constant control as (2.32) with $\delta = 0.5$ and analyse it on the phase plan. We suppose initial condition as (0.95,0.05,0) and $\beta = 2$, $\gamma = 0.4$ as rates values. From the previous theorem, we obtain the sliding mode exists surely if $0.43 \leq k \leq 0.49$. Observe the following figures, that reports the model simulation with threshold level firstly set to $k = 0.35$, which does not fall under the assumptions of the Proposition 2.2, and then $k = 0.45$.

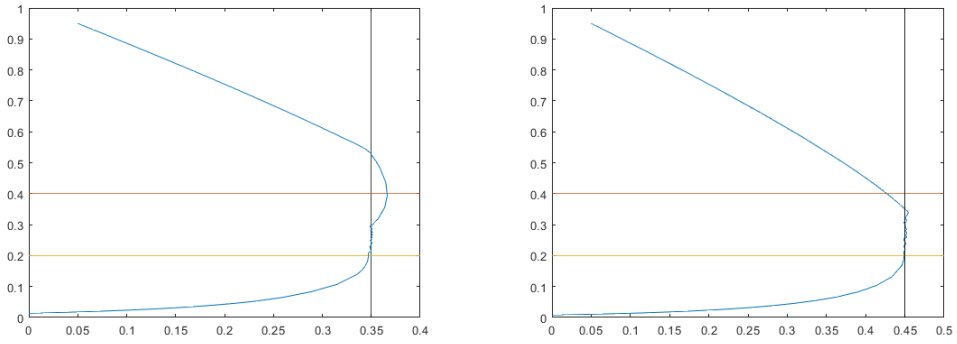

(a) (b)

Figure 2.10: Phase plan in which the *blue* curve is the solution, the *red* and *yellow* lines define the sliding domain boundary and the *black* line is $y = k$. On the left (a), $k = 0.35$ and the trajectory initially causes an outbreak in the controlled system, then decreases and hits the sliding region. Instead on the right side (b), $k = 0.45$ and the trajectory directly hits the domain.

For k value less than $1 - \gamma/(\delta\beta) + \gamma/\beta \ln(1/R_0^m)$, the curve of the infected will have a maximum peak greater than k, due to the fact that the value of the susceptibles when the curve of the infected reaches $y = k$ is too high and causes an outbreak of the epidemic. If k is set greater, then the solution enters in the sliding domain when the number of susceptibles is too low. Observe now the following figure, that reports the model simulation with a threshold level set to $k = 0.2$.

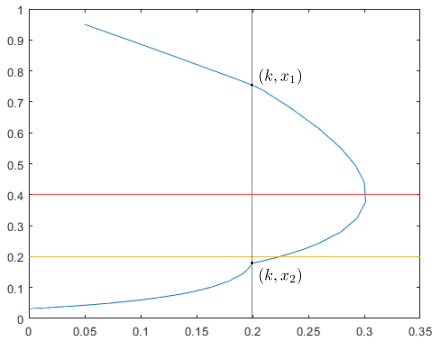

Figure 2.11: Modified SIR model with a piecewise constant control but no sliding mode.

The controlled system develops between the points (k, x_1) and (k, x_2) in the phase plan considered, where x_1 is a fraction of susceptibles at which the classical SIR infected curve reaches the threshold level and where x_2 is a fraction of susceptibles at which the modified SIR infected curve reaches the threshold level. We know that x_2 satisfies the following implicit relation

$$x_2 - \frac{\gamma}{\delta\beta} \ln(x_2) = x_1 + k - k - \frac{\gamma}{\delta\beta} \ln(x_1) \tag{2.41}$$

If we suppose $x_2 < \gamma/\beta$, then with the parameter used we obtain

$$x_2 - \frac{\gamma}{\delta\beta} \ln(x_2) = x_2 - 0.4 \ln(x_2) > 0.84 \tag{2.42}$$

since the function $x - 0.4 \ln(x)$ is monotonically decreasing for $x < 0.4$ and monotonically increasing for $x > 0.4$. We obtain also $x_1 - 0.4 \ln(x_1) > 0.84$ from (2.41). We proceed graphically, looking for the value greater than γ/β and we get $x_1 > 0.7$. Let us remember x_1 is a fraction of susceptibles at which the classical SIR infected curve reaches the threshold level, therefore it satisfies

$$x_1 - \frac{\gamma}{\beta} \ln(x_1) = x(0) + y(0) - k - \frac{\gamma}{\beta} \ln(x(0)) \tag{2.43}$$

With the previous condition we have

$$0.77 < x_1 - 0.2 \ln(x_1) = 1 - k - 0.2 \ln(x(0)) \Rightarrow k < 0.24 \tag{2.44}$$

Therefore no sliding mode will occur if the chosen threshold level k is below 0.24. For this particular simulation case, we've found the sliding mode exists if $0.24 \leq k \leq y_{max} = 0.49$.

Within this problem, we can also obtain the duration of the restrictive measures implementation. Since on the sliding mode region

$$\dot{x}(t) = -\gamma k \tag{2.45}$$

the resulting dynamics is

$$x(t) = x_1 - \gamma k t \tag{2.46}$$

where x_1, as said before, is the number of susceptibles when the infected curve meets the threshold level. By placing $x(T) = \gamma/\beta$ and $x_1 = \gamma/(\delta\beta)$, i.e. the end and starting points of the sliding region, we can get the duration of interventions being implemented

$$T = -\frac{1}{\gamma k}\left(\frac{\gamma}{\beta} - \frac{\gamma}{\delta\beta}\right) = -\frac{1}{\beta k}\left(1 - \frac{1}{\delta}\right) \tag{2.47}$$

With the values used in these simulations with a piecewise constant control, with an infected threshold level set by $k = 0.45$, the solution takes about $T = 1.1$ days to slide along the sliding mode region, and then return to the classical SIR model.

Non-constant control. We now consider an example of a discontinuous control action that is not constant, but dependent on the current fraction of the infected. Suppose $g(y) = 1 - y$ and resume the calculations of the *Filippov convex method* for the sliding mode region

$$\Omega = \left\{(x, y) \in \mathbb{R}^2 : \quad \frac{\gamma}{\beta} \leq x \leq \frac{\gamma}{\beta(1-k)^2}, \quad y = k\right\} \tag{2.48}$$

As said before, the sliding mode exists if there is a non empty sliding mode region Ω where the two adjacent vector fields point toward the manifold.

For this model with a piecewise continuous control we can only state that sliding mode will definitely not occur if $k > y_{max}$ for the same reasons as above, where y_{max} is the maximum fraction of infected of the classical SIR model.

Let us now analyse the scenarios in which the sliding motion occurs. We consider the previous simulation set-up but with the non constant control $g(y) = 1 - y$. In the following figures, we can observe the vector field along the solution on the phase plane with a threshold level set to $k = 0.46$ and its corresponding simulation.

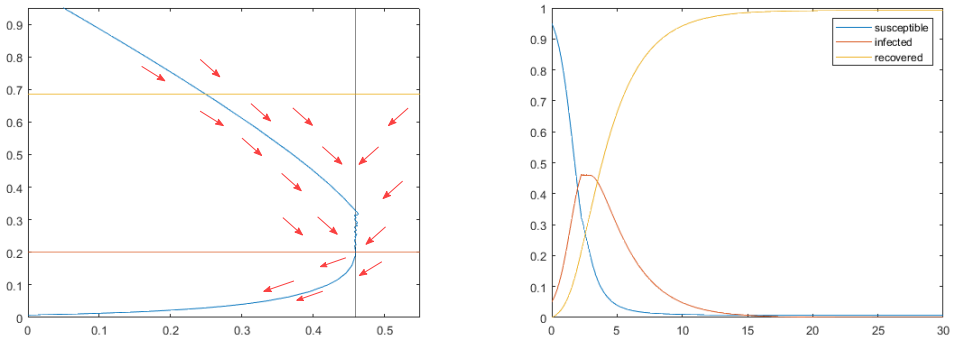

(a) (b)

Figure 2.12: The figure on the left (a) shows the vector field along orbit $x(y)$. The figure on the right (b), the model simulation is presented.

Even in this case, the solution can assume different behaviours. There will be trajectories that hit the sliding domain Ω directly, while others will cause an outbreak, then they will decrease and finally hit the sliding domain. On the basis of the characteristics of the original SIR, we can obtain the number of susceptibles x_1 when the infected curve reaches the threshold level $y = k$. Therefore x_1 satisfies

$$x_1 - \frac{\gamma}{\beta}\ln(x_1) = x_0 + y_0 - k - \frac{\gamma}{\beta}\ln(x_0) \tag{2.49}$$

If we suppose that the number of susceptibles when the infected curve reaches the threshold level x_1 is exactly equal to the first point of the sliding domain, that is

$$\left(k, \frac{\gamma}{\beta(1-k)^2}\right) \tag{2.50}$$

then we get that the threshold level k satisfies the following equation

$$\frac{\gamma}{\beta(1-k)^2} - \frac{\gamma}{\beta}\ln\left(\frac{\gamma}{\beta(1-k)^2}\right) = x_0 + y_0 - k - \frac{\gamma}{\beta}\ln(x_0) \tag{2.51}$$

By proceeding graphically or using the bisection or Newton methods, the selected value of k can be derived from the previous equation. This value corresponds to the situation in which the solution runs entirely through the sliding domain from the starting point of coordinates $(k, \gamma/\beta(1-k)^2)$, in the phase plan considered, to the end point $(k, \gamma/\beta)$.

Below we can observe two simulations of the modified SIR model with $g(y) = 1 - y$ and with two different values of the threshold level k but the same initial condition $(x(0), y(0), z(0)) = (0.95, 0.05, 0)$.

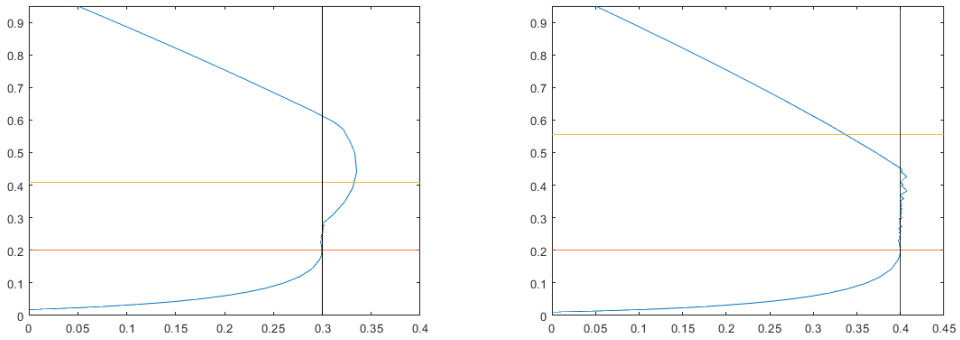

(a) (b)

Figure 2.13: Phase plan in which the *blue* curve is the solution, the *red* and *yellow* lines define the sliding domain boundary and the *black* line is $y = k$. On the left (a), there the phase plan in the case of $k = 0.3$, in which the trajectory initially causes an outbreak (number of infected exceeds k) and then decreases and hits the sliding domain. Instead on the right side (b) there is the second case with $k = 0.4$ but the trajectory directly hits the domain.

For the data set used for the simulations in this part, a k value of about 0.37 is obtained. Let us observe the system behaviour with this threshold level of infection.

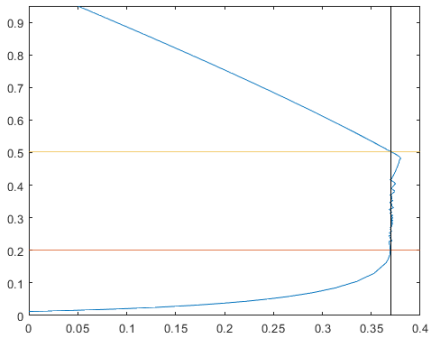

Figure 2.14: Phase plan in which the *blue* curve is the solution, the *red* and *yellow* lines define the sliding domain boundary and the *black* line is $y = k$.

If we consider this critical threshold value within our model, we can see that the solution does not have peaks above the threshold and runs entirely from its initial point through the sliding domain, within which the susceptible curve then decreases linearly as seen before, while the infected remain constant. As previously mentioned, it will happen that for k less than this critical value 0.37, the curve of the infected will have a maximum peak greater than k, due to the fact that the value of the susceptible when the curve of the infected reaches $y = 0.37$ is too high and causes an outbreak of the epidemic. If k is greater than 0.37, then the solution enters directly in the sliding domain.

2.4 Delayed control models

In typical applications, the information on the infection level is available only with some delay between the observation of the infected number and the implementation of lockdown policies. This motivates the introduction of a time delay in the control term $f(y)$. Therefore, in order to simulate a more realistic response to a disease, let us consider a delay $\tau > 0$. We can consider the modified version of the SIR model (2.2) with the delayed mitigation function

$$f(y(t)) = 1 - y(t - \tau), \quad \forall t \geq 0$$

This function will therefore be based not on the current fraction of infected but on its previous value of a certain time. We now report simulations of the modified model with the introduction of the delay in both behaviour cases of the SIR dynamics, with $\beta = 2$ and $\gamma = 0.4$ as epidemic rates. In the first simulations, the initial conditions are set to $(0.55, 0.45, 0)$ and the experimental set-up causes a modified effective reproduction number R_0^m below 1.

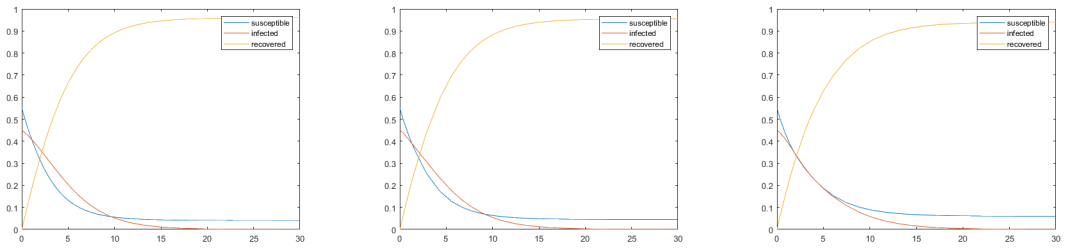

(a) (b) (c)

Figure 2.15: On the left, there is the simulation of modified SIR model with the effective reproduction number R_0^m below 1. The other figures show the simulations of the modified model with a time delay of 0.5 and 2 days in the control function.

Since $R_0^m < 1$, the infected curve is monotonically decreasing. The inclusion of a time delay τ in the control function of the modified model leads to an attenuation of the infection. This can be noticed from the number of final susceptibles which increases with the addition of the delay, while the fraction of final recovered decreases. This effect is amplified as the delay increases, thus suggesting an improvement in control when a time delay is introduced in the presence of a declining epidemic.

In the following case, the initial conditions are instead $(0.7, 0.3, 0)$ with the same epidemic rates as before. The infected curve, which is the solution of the modified SIR model, shows a unimodal trend.

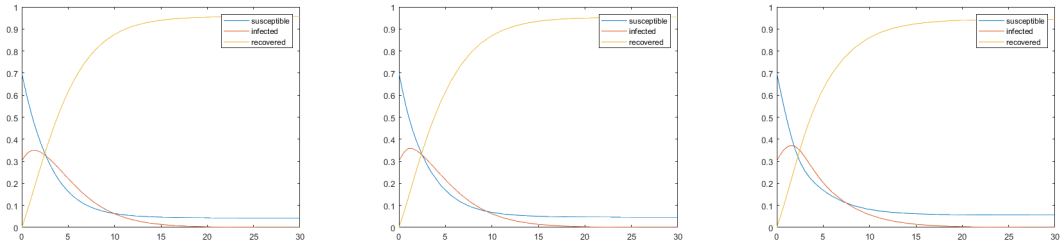

(a) (b) (c)

Figure 2.16: The left figure showa the modified SIR model with $R_0^m > 1$. The other figures show the modified model with a time delay of 0.5 and 2 days in the control function.

In this case, the effect of time delay introduction is twofold: initially, it leads to an increase in the peak of infection, while subsequently it smoothes the curve of the infected, leading to a steeper decline. In the simulations above, the infection peak increases from about 0.349 in the modified SIR model without delay to about 0.357 with a half-day delay and 0.37 with two days delay. At the same time the final number of susceptibles increases with respect to the case without delay time, as noted above.

Having observed the general effect of introducing a delay in the control function, let us now turn to a particular case. Below we report the simulations in the case in which the infected curve presents an unimodal behaviour in the original SIR model while it decreases monotonically to 0 in the modified version with $f(y) = 1-y$. Therefore we'll set the initial condition to $(0.85, 0.15, 0)$ and the infection and recover rates will be: $\beta = 0.6$ and $\gamma = 0.4$. So the basic reproduction number of the original SIR model is $R(0) = \beta x(0)/\gamma = 1.27$, instead of the model modified with the lockdown measure is $R(0) = \beta x(0)(1-y(0))^2/\gamma = 0.92$. Let us consider the delay of two days and observe the behaviour of the three models (classical, controlled and delayed control).

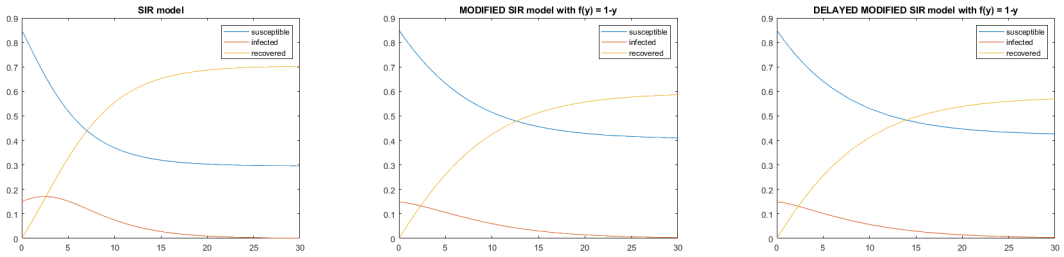

(a) (b) (c)

Figure 2.17: On the left, original SIR model with a $R_0 > 1$. In the middle, modified SIR model with $R_0^m < 1$. On the right, delayed control model with a delay of two days.

We could think that the insertion of delay in the model could cause the unimodal behaviour of the curve of the infected although it did not occur in the modified SIR model where the delay in the $f(y)$ function was not considered. However this phenomenon does not happen, in fact we can only observe a greater fraction of susceptibility at the final instant and that was what we were expecting based on the above considerations.

At this point, we could combine two concepts expressed during this first part on scalar models: the introduction of measures only in case a threshold level of infection is reached and the consideration of a time delay within the control. Therefore, let us study the SIR model with the addition of a piecewise continuous control function (2.22) and introduce the delay time in this case. We suppose the function $f(y)$ as

$$f(y(t)) = \begin{cases} 1 - y(t-\tau) & if \quad y(t-\tau) - k \geq 0 \\ 1 & if \quad y(t-\tau) - k < 0 \end{cases}$$

where k is the threhsold level of infected.

We initially decide to set $k = 0.37$, that was the critical value for the similar model without delay, studied before. Using the same initial conditions of the previous simulations without delay $(x(0), y(0), z(0)) = (0.95, 0.05, 0)$ and the same values for infection $\beta = 2$ and recover rates $\gamma = 0.4$, we obtain the following general behaviour.

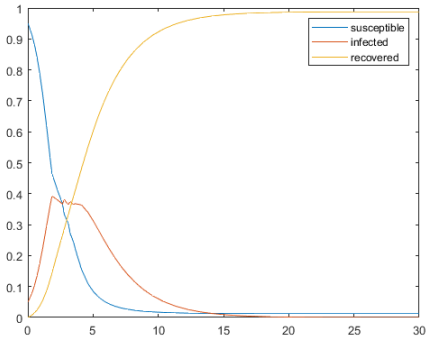

Figure 2.18: Simulation of the modified SIR model with a piecewise continuous control function and the introduction of the delay of $\tau = 0.1$ days.

However, let us focus on the solution of the phase plan with susceptibles on the vertical axis and infected on the orizontal axis and analyse its behaviour around the switching surface $y = k$.

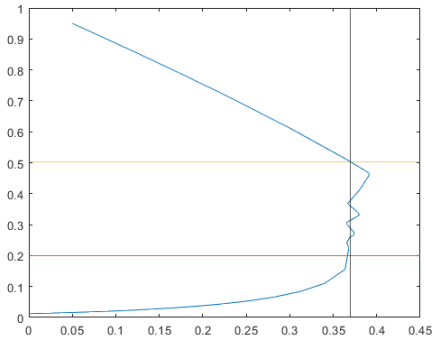

Figure 2.19: Phase plan with the solution of the modified SIR model with a piecewise continuous control function and the introduction of the delay of $\tau = 0.1$ days. The *blue* curve is the solution, the *red* and *yellow* lines define the sliding domain region and the *black* line is $y = k$.

Let us note that the trajectory of the system oscillates from one side to the other of the threshold surface $y = k$ that delimits the two types of model, giving rise to the so-called *chattering phenomenon* in which there is no perfect slipping along the sliding domain but a continuous crossing from one model to another. We can also note that the amplitude of these oscillations is the smaller the delay considered in the observation of the infected. The *chattering phenomenon* occurs when the delay is such to guarantee the existence of the sliding domain. A condition to be taken into account is surely that the delay is at least less than about half of the duration of interventions.

Chapter 3

Network SIR Model

In this chapter we study versions of the networked SIR model. We consider a population split into a set of nodes $\mathcal{V} = \{1, ..., n\}$, that represent different subpopulations, geographical areas or age ranges. The links $\mathcal{E} = \{(i, j) : i, j \in \mathcal{V}\}$ allow the potential spread of the disease. The interaction among subpopulations is described through a weighted graph $\mathcal{G} = (\mathcal{V}, \mathcal{E}, A)$, where A is the weight matrix and its entries a_{ij} embody the strength of the interaction between individuals of subpopulation i and subpopulation j. The presence of a link indicates a contact between the two nodes that may result from geographic or age proximity. Each individual node will have an own fraction of susceptible, infected and recovered and the transitions between these states, as a result of a contact, works as before. It is now clear that the topoplogy of the network will play a key role in defining the dynamics and we will focus precisely on this kind of analysis before introducing changes to the original system. We will initially report a general result available in the literature that expresses new threshold conditions for the dynamics combining the initial conditions, the infection parameters and the graph characteristics. We will dwell on the case of two nodes network, first deriving a corollary that makes the conditions of the theorem, mentioned before, more explicit and interpretable in this particular case, and then presenting numerical simulations. We will investigate a particular scenario of contact between a first population with an initial fraction of infected and a second totally susceptible population. For specific experimental set-ups, this will lead to the occurrence of a second infection peak in the first node. We will present numerical simulations also on networks with a larger number of nodes and different structures. Finally we discuss three control versions of the SIR network model.

Let us now start with the introduction of the classical SIR model applied to a graph of n nodes with a weight matrix A with entries a_{ij}

$$\begin{cases} \dot{x}_i(t) = -\beta x_i(t) \sum_{j=1}^{n} a_{ij} y_j(t) \\ \dot{y}_i(t) = \beta x_i(t) \sum_{j=1}^{n} a_{ij} y_j(t) - \gamma y_i(t) \\ \dot{z}_i(t) = \gamma y_i(t) \end{cases} \tag{3.1}$$

where, as previously said, β and γ are respectively infection and recover rate. Note that

the third equation is redundant because of the constraint $x_i(t)+y_i(t)+z_i(t) = 1, \forall i = 1..n$. We can rewrite the system in vectorial form as

$$\begin{cases} \dot{x}(t) = -\beta diag(x(t))Ay(t) \\ \dot{y}(t) = \beta diag(x(t))Ay(t) - \gamma y(t) \end{cases} \tag{3.2}$$

where $x(t), y(t), z(t) \in \mathbb{R}^n$ indicate vectors of susceptibles, infected and recovered at time t in all nodes, while $diag(x(t))$ is the diagonal matrix with fraction of susceptibles in all nodes as entries. At this point we proceed to the actual analysis of the dynamic behaviour of the model in the network case, starting from a result, strongly linked to the structure of the graph, presented in Mei et al. [5] and reported below. In stating the following theorem, we shall adopt the notation that any inequality between vectors is to be understood element by element and $\mathbf{1}_n = [1, ...,1]^T$, $\mathbf{0}_n = [0, ...,0]^T$.

Theorem 3.1. *Consider the network SIR model (3.1) over a strongly connected graph with weight matrix A. For $t \geq 0$, let $\lambda_{max}(t)$ and $v_{max}(t)$ be the dominant eigenvalue of the non-negative matrix $diag(x(t))A$ and the corresponding normalized left eigenvector, respectively. The following statements hold:*

1. *if $y(0) > \mathbf{0}_n$, and $x(0) > \mathbf{0}_n$, then*
   - *a) $t \mapsto x(t)$ and $t \mapsto y(t)$ are strictly positive for all $t \geq 0$,*
   - *b) $t \mapsto x(t)$ is monotonically decreasing, and*
   - *c) $t \mapsto \lambda_{max}(t)$ is monotonically decreasing;*
2. *the set of equilibrium points is the set of pairs $(x^*, \mathbf{0}_n)$, for any $x^* \in [0,1]^n$, and the linearisation of the network SIR model about $(x^*, \mathbf{0}_n)$ is*

$$\begin{cases} \dot{x}(t) = -\beta diag(x^*)Ay \\ \dot{y}(t) = \beta diag(x^*)Ay - \gamma y \end{cases} \tag{3.3}$$

3. *(behaviour below the threshold) let the time $\tau \geq 0$ satisfy $\beta\lambda_{max}(\tau) < \gamma$. Then the weighted average $t \mapsto v_{max}(\tau)^T y(t)$, for $t \geq \tau$, is monotonically and exponentially decreasing to zero;*
4. *(behaviour above the threshold) if $\beta\lambda_{max}(0) > \gamma$ and $y(0) > \mathbf{0}_n$, then,*
   - *a) (epidemic outbreak) for small time, the weighted average $v_{max}(0)^T y(t)$ grows exponentially fast with rate $\beta\lambda_{max}(0) - \gamma$, and*
   - *b) there exists $\tau > 0$ such that $\beta\lambda_{max}(\tau) < \gamma$;*
5. *each trajectory converges asymptotically to the equilibrium point, $\lim_{t\to\infty} y(t) = \mathbf{0}_n$, so that the epidemic asymptotically disappears.*

Proof. Regarding statement 1a), $x(t) > \mathbf{0}_n$ is due to the fact that Ay is bounded and $x(t)$ is continously differentiable to t. The statement that $y(t) > \mathbf{0}_n$ for all $t > 0$ is proved as a consequence of Nagumo's Theorem; while statement 1b) is due to the fact that $\dot{x}_i(t)$

being strictly negative. From statement 1a) we know that each $x_i(t)$ is positive, and from A being irreducible and $y(0) \neq \mathbf{0}_n$ we know that $\sum_{j=1}^n a_{ij}y_j$ is positive. Therefore, $\dot{x_i}(t) = -\beta x_i(t) \sum_{j=1}^n a_{ij}y_j(t) < 0$ for all $i = 1...n$ and $t \geq 0$.

For statement 1c), we start by recalling the following property on the spectral radius: for B and C nonnegative square matrices, if $B \leq C$, then $\rho(B) \leq \rho(C)$. Now, pick two time instances t_1 and t_2 with $0 < t_1 < t_2$. Let $\alpha = \max_i x_i(t_2)/x_i(t_1)$ and note $0 < \alpha < 1$ because $x(t)$ is strictly positive and monotonically decreasing. Now note that,

$$diag(x(t_1))A > \alpha\, diag(x(t_1))A \geq diag(x(t_2))A,$$

so that, using this property above, we know

$$\rho(diag(x(t_1))A) > \alpha\rho(diag(x(t_1))A) \geq \rho(diag(x(t_2))A).$$

This concludes the proof of statement 1c).

Regarding argument 2), note that a point (x^*, y^*) is an equilibrium if and only if:

$$\begin{aligned} \mathbf{0}_n &= -\beta diag(x^*)Ay^*, \quad and \\ \mathbf{0}_n &= \beta diag(x^*)Ay^* - \gamma y^* \end{aligned}$$

Therefore, each point of the form $(x^*, \mathbf{0}_n)$ is an equilibrium. On the other hand, summing the last two equalities we obtain $\mathbf{0}_n = \gamma y^*$ and thus y^* must be $\mathbf{0}_n$. As a straightforward result, the linearization of model (3.1) about any equilibrium point $(x^*, \mathbf{0}_n, \mathbf{1}_n - x^*)$ is given by equation (3.3). Regarding statement 3), multiplying $v_{max}(\tau)^T$ from the left on both sides of the model in matrix form, we obtain:

$$\begin{aligned} \frac{d}{dt}(v_{max}(\tau)^T y(t)) &= v_{max}(\tau)^T \left(\beta diag(x(t))Ay(t) - \gamma y(t)\right) \\ &\leq v_{max}(\tau)^T \left(\beta diag(x(\tau))Ay(t) - \gamma y(t)\right) \\ &= (\beta\lambda_{max}(\tau) - \gamma)v_{max}(\tau)^T y(t) \end{aligned}$$

Therefore, we get

$$v_{max}(\tau)^T y(t) \leq (v_{max}(\tau)^T y(0))e^{(\beta\lambda_{max}(\tau)-\gamma)t}$$

The right-hand side exponentially decays to zero when $\beta\lambda_{max}(\tau) < \gamma$. Therefore, $v_{max}(\tau)^T y(t)$ also decreases monotonically and exponentially to zero for all $t \geq \tau$. Regarding statement 4a), note that based on the argument in 1a), we only need to consider the case when $y(0) > \mathbf{0}_n$. Left-multiplying $v_{max}(0)^T$ on both sides of equation (3.3), we obtain:

$$\begin{aligned} \frac{d}{dt}(v_{max}(0)^T y(t))|_{t=0} &= v_{max}(0)^T \left(\beta diag(x(t))Ay(t) - \gamma y(t)\right)|_{t=0} \\ &= (\beta\lambda_{max}(0) - \gamma)v_{max}(0)^T y(0) \end{aligned}$$

Since $\beta\lambda_{max}(0) - \gamma > 0$, the initial time derivative of $v_{max}(0)^T y(t)$ is positive. Since $t \mapsto v_{max}(0)^T y(t)$ is a continously differentiable function, there exists $\tau' > 0$ such that $\frac{d}{dt}(v_{max}(0)^T y(t)) > 0$ for any $t \in [0, \tau']$. Regarding statement 4b), since $\dot{x}(t) \leq \mathbf{0}_n$ and is lower bounded by $\mathbf{0}_n$, we conclude that the limit $\lim_{t\to\infty} x(t)$ exists. Moreover, since $x(t)$ is

monotonically non-increasing, we have $\lim_{t\to\infty} \dot{x}(t) = 0$, which implies either $\lim_{t\to\infty} x(t) = \mathbf{0}_n$ or $\lim_{t\to\infty} y(t) = \mathbf{0}_n$. If $x(t)$ converges to $\mathbf{0}_n$, then $\dot{y}(t)$ converges to $-\gamma y(t)$. Therefore, there exists $T > 0$ such that $\beta\lambda_{max}(T) < \gamma$, which leads to $y(t) \to \mathbf{0}_n$ as $t \to +\infty$; If $x(t)$ converges to some $x^* > \mathbf{0}_n$, then $y(t)$ still converges to $\mathbf{0}_n$. Therefore, for any $(x(0), y(0))$, the trajectory $(x(t), y(t))$ converges to some equilibria with the form $(x^*, \mathbf{0}_n)$, where $x^* \geq \mathbf{0}_n$. Let

$$x(t) = x^* + \delta_x(t) \quad and \quad y(t) = \mathbf{0}_n + \delta_y(t)$$

We know that $\delta_x(t) \geq 0$ and $\delta_y(t) \geq 0$ for all $t \geq 0$. Moreover, $\delta_x(t)$ is monotonically non-increasing and converges to $\mathbf{0}_n$, and there exists $T > 0$ such that, for any $t \geq T$, $\delta_y(t)$ is monotonically non-increasing and converges to $\mathbf{0}_n$. Let λ^* and v^* denote the dominant eigenvalue and the corresponding normalized left eigenvector of matrix $diag(x^*)A$, respectively, that is, ${v^*}^T diag(x^*)A = \lambda^* {v^*}^T$. First let us suppose $\beta\lambda^* - \gamma > 0$, then the linearized system around $(x^*, \mathbf{0}_n)$ is written as

$$\dot{\delta}_x = -\beta diag(x^*)A\delta_y$$
$$\dot{\delta}_y = \beta diag(x^*)A\delta_y - \gamma\delta_y$$

Since $\beta\lambda^* - \gamma > 0$, the linearized system is exponentially unstable, which contradicts the fact that $(\delta_x(t), \delta_y(t)) \to (\mathbf{0}_n, \mathbf{0}_n)$ as $t \to +\infty$. Alternatively, suppose $\beta\lambda^* - \gamma = 0$. By left multiplying ${v^*}^T$ on both sides of the equation for $\dot{y}(t)$ in the scalar model, we obtain

$${v^*}^T \dot{\delta}_y = (\beta\lambda^* - \gamma)({v^*}^T \delta_y) + \beta {v^*}^T diag(\delta_x)A\delta_y = \beta {v^*}^T diag(\delta_x)A\delta_y > \mathbf{0}_n$$

which contradicts $\delta_y(t) \to \mathbf{0}_n$ as $t \to +\infty$. Therefore, we conclude that $\beta\lambda^* - \gamma < 0$. Since $\lambda_{max}(t)$ is continous on t, we conclude that exists $\tau < +\infty$ such that $\beta\lambda_{max}(\tau) - \gamma < 0$. □

On the basis of the previous theorem, the effective reproduction number in the deterministic network SIR model is $R(t) = \beta\lambda_{max}(t)/\gamma$. When $R(0) > 1$, we have an epidemic outbreak, i.e. an exponential growth of infected individual for the inital time interval. In any case, the theorem guarantees that, after at most finite time, $R(t)$ becomes less than 1 and the infected population decreases exponentially fast to zero.

Now we can turn into a more targeted analysis, focusing on graphs composed of initially a few nodes in which we will show some non-classical and unexpected phenomena that can occur in particular scenarios.

3.1 SIR model on a two nodes network

The previous theorem is generic and provides a result regarding the dynamic behaviour of the SIR model on a network in general. Let us now specialize on an indirect network composed by only two nodes $\mathcal{V} = \{1,2\}$. As a first network interpretation, we can assume that the two nodes reflect a distinction of the population by geographical areas, where

therefore contacts between individuals belonging to the same node are different from those between individuals from different areas. In particular, we assume that the second type of contact is disadvantaged compared to the first, underlining the geographical distance.

This can be translated into the SIR model reported below over an indirect graph consisting of only two nodes.

$$\begin{cases} \dot{x}_i(t) = -\beta x_i(t)(a_{i1}y_1(t) + a_{i2}y_2(t)) \\ \dot{y}_i(t) = \beta x_i(t)(a_{i1}y_1(t) + a_{i2}y_2(t)) - \gamma y_i(t) \end{cases} \qquad i = 1,2 \tag{3.4}$$

where the third equation on recovered has been omitted as redundant. For this network, we consider the following symmetric weight matrix

$$A = \begin{bmatrix} 1 & 1-\epsilon \\ 1-\epsilon & 1 \end{bmatrix} \tag{3.5}$$

in which the interaction between the two nodes is weakened by the constant $\epsilon \in [0,1]$. This term is related to the distance between the two areas, so as to differentiate the contacts between one node's susceptibles and other node's infected. If $\epsilon = 0$, then the two nodes actually represent a kind of virtual subdivision of a single population, since the dynamics is the same. If, on the other hand, $\epsilon = 1$ then the two nodes are no longer connected, but totally separated and the analysis of their dynamics falls back into the scalar model theory in both cases.

Corollary 3.1.1. *Consider the SIR network model (3.4) on a graph composed by two nodes with a weight matrix A defined as (3.5). If the following conditions hold*

$$\begin{cases} \frac{\beta}{\gamma}(x_1(0) + x_2(0)) < 2 \\ \frac{\beta}{\gamma}(x_1(0) + x_2(0)) - \frac{\beta^2}{\gamma^2}x_1(0)x_2(0)(2\epsilon - \epsilon^2) < 1 \end{cases} \tag{3.6}$$

then the weighted average of $y(t)$, $v_{max}(0)^T y(t)$ for $t \geq 0$, is monotonically and exponentially decreasing to zero. Otherwise it is initially exponentially increasing and then it decreases to zero.

Proof. Considering a generic $\epsilon \in (0,1)$, let us now characterise the elements of the previous theorem for this particular system. We start with the matrix that is a combination of the fraction of susceptibles at each node and the contact between the two nodes.

$$diag(x(t))A = \begin{pmatrix} x_1(t) & (1-\epsilon)x_1(t) \\ (1-\epsilon)x_2(t) & x_2(t) \end{pmatrix} \tag{3.7}$$

whose characteristic polynomial is $(x_1(t) - \lambda)(x_2(t) - \lambda) - (1-\epsilon)^2 x_1(t)x_2(t) = 0$.
We can derive the eigenvalues of this matrix, in which time dependency is maintained and we obtain that

$$\lambda_{1,2}(t) = \frac{x_1(t) + x_2(t)}{2} \pm \sqrt{\left(\frac{x_1(t) + x_2(t)}{2}\right)^2 - (2\epsilon - \epsilon^2)x_1(t)x_2(t)} \tag{3.8}$$

Since the matrix $diag(x(t))A$ is positive, then the eigenvalue with the largest real part is real and corresponds to a strictly positive eigenvector. Therefore, we can state that

$$\lambda_{max}(t) = \frac{x_1(t)+x_2(t)}{2} + \sqrt{\left(\frac{x_1(t)+x_2(t)}{2}\right)^2 - (2\epsilon-\epsilon^2)x_1(t)x_2(t)} \tag{3.9}$$

It remains to find the explicit expression of $v_{max}(t)$, i.e. the normalised left eigenvector corresponding to the dominant eigenvalue for this case. Proceeding with the calculations, we get that

$$v_{max}(t) = \left(\frac{(1-\epsilon)x_2(t)}{(1-\epsilon)x_2(t)+\lambda_{max}(t)-x_1(t)}, \frac{\lambda_{max}(t)-x_1(t)}{(1-\epsilon)x_2(t)+\lambda_{max}(t)-x_1(t)}\right)^T \tag{3.10}$$

The Theorem 3.1 for the dynamic behaviour of the SIR-network model states that if there is a time $\tau \geq 0$ where $\beta\lambda_{max}(\tau) < \gamma$, then the weighted average $t \mapsto v_{max}(\tau)^T y(t)$, for $t \geq \tau$, is monotonically and exponentially decreasing to 0. This means that if the condition is respected, then the generic equilibrium point of the system $(x^*, \mathbf{0}_2)$ with $x^* \in [0,1]^2$ is locally stable. We rewrite the condition using the expression found for $\lambda_{max}(t)$.

$$\beta\frac{x_1(t)+x_2(t)}{2} + \beta\sqrt{\left(\frac{x_1(t)+x_2(t)}{2}\right)^2 - (2\epsilon-\epsilon^2)x_1(t)x_2(t)} < \gamma$$
$$\frac{\beta}{\gamma}\sqrt{\left(\frac{x_1(t)+x_2(t)}{2}\right)^2 - (2\epsilon-\epsilon^2)x_1(t)x_2(t)} < 1 - \frac{\beta}{\gamma}\frac{x_1(t)+x_2(t)}{2}$$

This inequality with radical translates into the following three equations system

$$\begin{cases} \left(\frac{x_1(t)+x_2(t)}{2}\right)^2 - (2\epsilon-\epsilon^2)x_1(t)x_2(t) \geq 0 \\ 1 - \frac{\beta}{\gamma}\frac{x_1(t)+x_2(t)}{2} > 0 \\ \frac{\beta^2}{\gamma^2}\left[\left(\frac{x_1(t)+x_2(t)}{2}\right)^2 - (2\epsilon-\epsilon^2)x_1(t)x_2(t)\right] < 1 - 2\frac{\beta}{\gamma}\frac{x_1(t)+x_2(t)}{2} + \frac{\beta^2}{\gamma^2}\left(\frac{x_1(t)+x_2(t)}{2}\right)^2 \end{cases}$$

where the first inequality is always verified since λ_{max} is real. Rewrite the last two conditions that will be equal to $\beta\lambda_{max}(t) < \gamma$ in the case of a network consisting of two nodes and the particular weight matrix A we have defined.

$$\beta\lambda_{max}(t) < \gamma \quad \Leftrightarrow \quad \begin{cases} \frac{\beta}{\gamma}(x_1(t)+x_2(t)) < 2 \\ \frac{\beta}{\gamma}(x_1(t)+x_2(t)) - \frac{\beta^2}{\gamma^2}x_1(t)x_2(t)(2\epsilon-\epsilon^2) < 1 \end{cases} \tag{3.11}$$

We have therefore found specific expressions for the determination of average dynamics in the two nodes network model. Consider *Point 3)* of the Theorem 3.1 on the behaviour below threshold, setting $\tau = 0$, so we can state that if the two previous conditions are fulfilled at the initial instant $t = 0$, then the weighted average $v_{max}(0)^T y(t)$ is monotonically and exponentially decreasing at 0. It can be verified that a strict violation of one or both of the previous conditions leads to an instability of the equilibrium point $(x^*, \mathbf{0}_2)$, i.e. an initial increasing trend in the weighted average of the infected curve $v_{max}(0)^T y(t)$.

□

3.1.1 Initial infection in both nodes

Let us observe the behaviour of the weighted average of the three categories of susceptible, infected and recovered. For the simulations below, the set-up includes the following values for infection and recover rate respectively: $\beta = 0.7$ and $\gamma = 0.55$, while assuming the distance term $\epsilon = 0.2$. As for the scalar model, we simulate both behaviours of the average infected curve: in the first case, the initial conditions on the nodes are $(x_1(0), y_1(0), z_1(0)) = (0.25, 0.75, 0)$ and $(x_2(0), y_2(0), z_2(0)) = (0.6, 0.4, 0)$, while for the second case, we have set $(x_1(0), y_1(0), z_1(0)) = (0.75, 0.25, 0)$ and $(x_2(0), y_2(0), z_2(0)) = (0.95, 0.05, 0)$; therefore assuming the initial presence of infected individuals in both nodes.

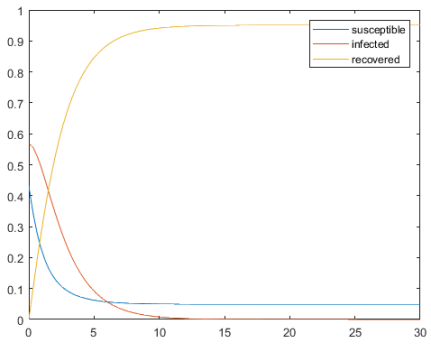

Figure 3.1: Simulation of average behaviour of the original SIR model on indirect graph consists of only two nodes with $\beta\lambda_{max}(0) < \gamma$.

With the parameters and initial conditions chosen for the first case, through calculations we can see that the two conditions of the Corollary 3.1.1 are satisfied. As we can see from the graph above, the average behaviour of the three groups is consistent with what we expected from the previous theorem. As regards the second case, on the other hand, both conditions in (3.6) are not respected.

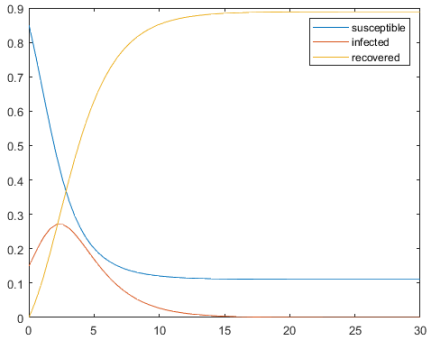

Figure 3.2: Simulation of average behaviour of the original SIR model on indirect graph consists of only two nodes with $\beta\lambda_{max}(0) > \gamma$.

Based on the general theorem presented earlier, the previous figure illustrates the behaviour of the average susceptible, average infected and average recovered quantities starting from an initial infection fraction in both nodes and with the reproduction number for the network model above 1 at time 0. The evolution of the average infected curve shows an initial exponential growth, like in the scalar model.

The theorem presented above for the SIR-network provides a parallel result to that for the classical SIR. However, underneath the average behaviour there may be hidden phenomena on the dynamics at individual nodes that are different from those expected. We will consider the dynamics from the perspective of each node and for this purpose, we recall the scalar definition of their effective reproduction numbers

$$R_{0i} = \frac{\beta}{\gamma} x_i(0) \quad i = 1,2$$

We are interested in investigating the dynamics in the nodes individually in the two different situations: firstly, where the average behaviour of the infected curve would show a decreasing trend; and then, where the average infected displays a unimodal dependence on time. Let us therefore observe the simulations in the two different cases studied before, with the same sets of initial conditions and epidemic rates.

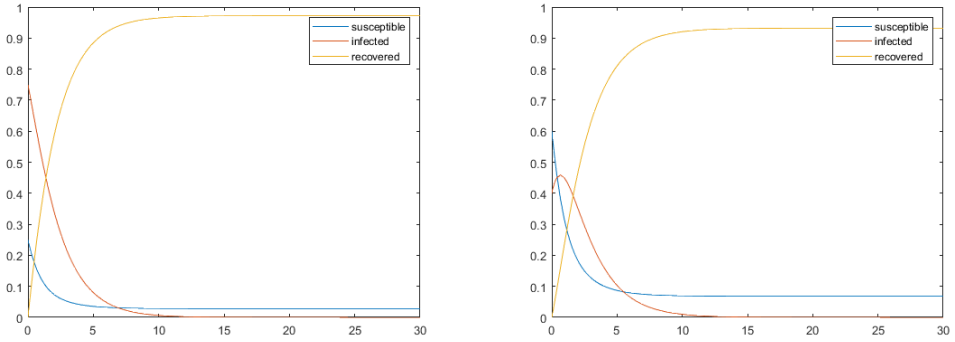

(a) (b)

Figure 3.3: Simulation of the original SIR model on the two nodes network with initial condition $(0.25, 0.75, 0)$ on the left and $(0.6, 0.4, 0)$ on the right. The infection and recovery rates used have the following values respectively: $\beta = 0.7$ and $\gamma = 0.55$, while $\epsilon = 0.2$.

In this first simulation, the dynamics in the left node are as expected, given the low initial number of susceptibles in that node (a sign of advanced development of the infection); whereas in the second node, although the classic reproduction number R_{02} is initially less than 1, proximity to a seriously infected node leads the curve of the infected to increase initially.

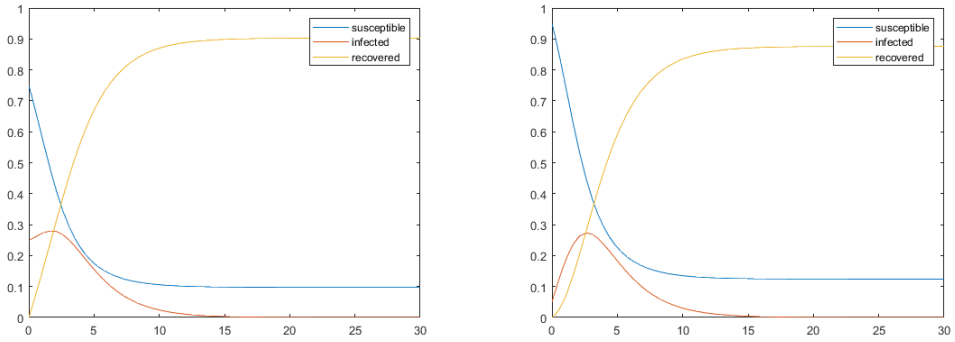

(a) (b)

Figure 3.4: Simulation of the original SIR model on the two nodes network with initial condition $(0.7, 0.3, 0)$ on the left and $(0.95, 0.05, 0)$ on the right. The infection and recovery rates used have the following values respectively: $\beta = 0.7$ and $\gamma = 0.55$, while $\epsilon = 0.2$.

The considerations in this second simulation are very similar to those in the previous case: the first node, given the encounter with the second (despite the fact that it has a very low initial rate of infected), shows the curve of the initially growing infected; whereas the second node shows the expected behaviour from the scalar dynamics.

3.1.2 Initial infection in only one node

In this part we want to focus on the investigation of the SIR-network model in a particular case study: only one node has a fraction of infected people and at least one of the conditions in (3.6) is strictly violated. Therefore, in the scenario studied, the Theorem 3.1 predicts a unimodal behaviour of the average curve of the infected of the system. We want to analyse the model where the network simulates a contact between two sub-populations in which initially one is totally susceptible and without infection. The previous conditions concern the general behaviour of the system, however for this case, we would like to analyse the dynamics of the SIR in the nodes separately, as done for the previous simulations. Assuming that the infection rate β is greater than the recover one γ, we will have that

$$R_{01} = \frac{\beta}{\gamma} x_1(0) \quad \textit{and} \quad R_{02} = \frac{\beta}{\gamma} x_2(0) = \frac{\beta}{\gamma} > 1$$

Since the first derivative of $y_2(t)$ at $t = 0$ is

$$\begin{aligned} \dot{y}_2(0) &= \beta x_2(0)((1-\epsilon)y_1(0) + y_2(0)) - \gamma y_2(0) \\ &= \beta(1-\epsilon)y_1(0) > 0 \end{aligned}$$

Then the behaviour of the SIR model in the second node is as follows: the curve of the susceptible is monotonically decreasing starting from 1, while the curve of the infected shows an initially increasing trend (due to the interaction with the infected of the first

node who bring the infection to the second node), reaching the peak and then decreasing at 0. This is the dynamic behaviour observed regardless of the initial conditions of the first node, as long as there is a fraction of infected greater than 0.

Regarding the node with the initial infection, different cases can occur depending on the set of parameters (i.e. infection rate, recover rate and initial conditions) used within the model. Its initial first derivative of the infected curve is

$$\begin{aligned}\dot{y_1}(0) &= \beta x_1(0)(y_1(0) + (1-\epsilon)y_2(0)) - \gamma y_1(0) \\ &= y_1(0)(\beta x_1(0) - \gamma)\end{aligned}$$

Therefore, if $R_{01} > 1$, then the behaviour of $y_1(t)$ is unimodal as in the scalar case. The infected curve is initially increasing and then after the peak, it decreases exponentially to 0, falling into the predictable behaviour from the traditional SIR in the scalar case. We can observe that the first derivative shows an initial increasing trend.

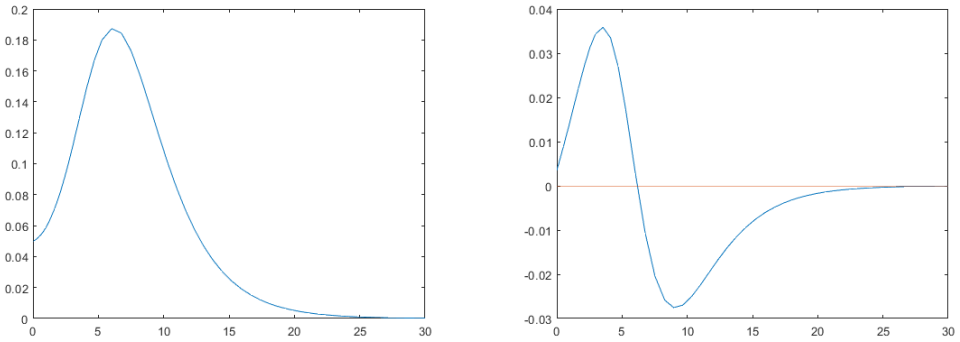

(a) (b)

Figure 3.5: Simulation of the original SIR model on the first node, with an initial conditions as $(x_1(0), y_1(0), z_1(0)) = (0.95, 0.05, 0)$ with the infection and recovery values respectively: $\beta = 0.6$ and $\gamma = 0.5$. The distance term ϵ is set to 0.2. On the left, there's the curve of infected $y_1(t)$, while on the right hand, the figure shows its first derivative $\dot{y_1}(t)$.

On the other hand, if $R_{01} < 1$, then two different behaviours of the first node infected curve $y_1(t)$ may occur. For values close to 1 or an high distance term ϵ, there is the occurrence of an atypical behaviour of the infected curve: the first derivative starts out negative but its maximum peak is positive. This means that the infected curve is initially decreasing; following the first point at which $\dot{y_1}$ is zero the curve y_1 changes trend. It becomes increasing to a peak of infection, and then decreasing to 0, after the second point at which the first derivative is zero.

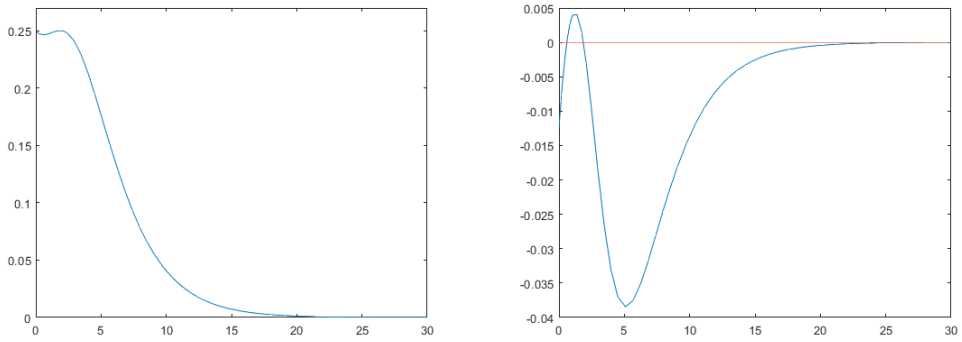

(a) (b)

Figure 3.6: Simulation of the original SIR model on the first node, with an initial conditions as $(x_1(0), y_1(0), z_1(0)) = (0.8, 0.2, 0)$ with the infection and recovery values respectively: $\beta = 0.6$ and $\gamma = 0.5$. The distance term ϵ is set to 0.2. On the left, there's the curve of infected $y_1(t)$, while on the right hand, the figure shows its first derivative $\dot{y_1}(t)$.

Instead, for lower values of the classical effective reproduction number R_{01}, the infected curve y_1 is always decreasing, in fact the first derivative remains negative. If the reproduction number further decreases, the curve becomes exponentially decreasing as in the scalar model.

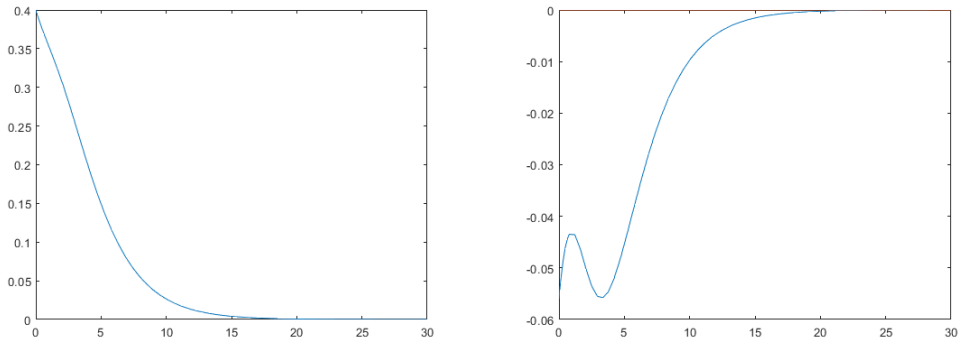

(a) (b)

Figure 3.7: Simulation of the original SIR model on the first node, with an initial conditions as $(x_1(0), y_1(0), z_1(0)) = (0.6, 0.4, 0)$ with the infection and recovery values respectively: $\beta = 0.6$ and $\gamma = 0.5$. The distance term ϵ is set to 0.2. On the left, there's the curve of infected $y_1(t)$, while on the right hand, the figure shows its first derivative $\dot{y_1}(t)$.

In the previous simulations, we kept the infection and recovery rates and the distance term between the two nodes constant by changing the initial conditions on the first node. The analysis shows that the first derivative of the infected curve of the first node y_1 has at most two points where it nulls out, which brings to light a singular and atypical

phenomenon compared to the traditional hypothesis concerning the SIR model. In fact, we consider a population characterized by a small initial fraction of infected people, such as to cause an exponential decrease to 0, using the scalar SIR model theory. However, if this first population meets a totally healthy one, it begins to infect it and then suffers a *return wave of infection*. This means that the curve of the infected of the first population, instead of decreasing as it would if it were isolated, causes an outbreak of the epidemic with a second peak of infection (the first one is in initial condition) and then returns to decrease.

3.1.3 Effect of distance term ϵ

At this point it is interesting to observe the behaviour of the curve y_1 analysed above as the distance term ϵ varies; given our interest, at a later stage of our analysis, in integrating measures of limiting social interactions into the model as done for the scalar case. Let us therefore suppose that we vary the distance parameter ϵ between 0 and 1, moving from a network in which inter-nodal interaction is maximised to a situation in which such contact is gradually weakened with respect to interaction within the same node. We first assume that we start (in the case $\epsilon = 0$) from a combination of the initial parameters such that the infected curve shows an epidemic outbreak and observe its change as contact with the second node weakens. Next, we will start instead from a situation in which the atypical phenomenon, mentioned earlier, occurs; and finally, the situation analysed is one in which for low ϵ values, the infected curve shows a decreasing behaviour.

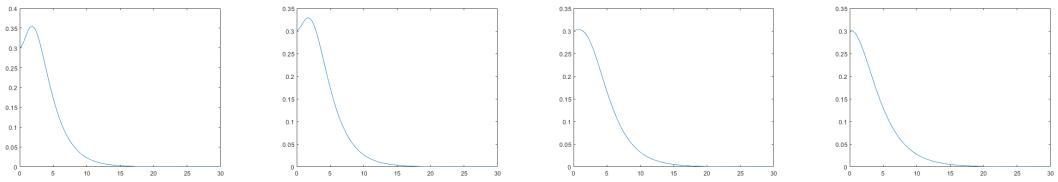

(a) (b) (c) (d)

Figure 3.8: Simulation of the original SIR model on the first node, with an initial conditions as $(x_1(0), y_1(0), z_1(0)) = (0.7, 0.3, 0)$ with the infection and recovery values respectively: $\beta = 0.75$ and $\gamma = 0.5$. The distance term ϵ is set, starting from the left, to $0, 0.2, 0.5, 1$.

We can see that, given the same initial conditions at the first node and the same infection and recover rates, increasing the distance term ϵ leads to a smoothing of the curve of the infected y_1, i.e. a decrease in the value of the infection peak and a shortening of the interval in which this curve is increasing. Despite the increase in distance term, which further leads to a weakening of the interaction between the two nodes, the curve maintains its initially increasing and then decreasing trend.

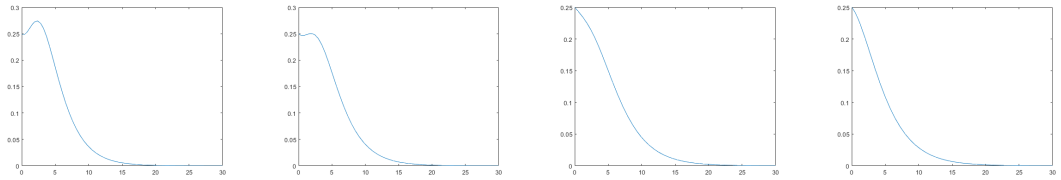

(a) (b) (c) (d)

Figure 3.9: Simulation of the original SIR model on the first node, with an initial conditions as $(x_1(0), y_1(0), z_1(0)) = (0.75, 0.25, 0)$ with the infection and recovery values respectively: $\beta = 0.6$ and $\gamma = 0.5$. The distance term ϵ is set, starting from the left, to $0, 0.2, 0.5, 1$.

As we can observe in this case, the atypical phenomenon occurs where $\epsilon = 0$ and $\epsilon = 0.2$, after that the attenuation of the inter-nodal interaction and, consequently, of the first derivative leads to a change in the behaviour of the y_1 curve. For higher values of ϵ, i.e. for situations where the nodes are strongly closed with little interaction with the outside, the infected curve becomes decreasing throughout the simulation time interval.

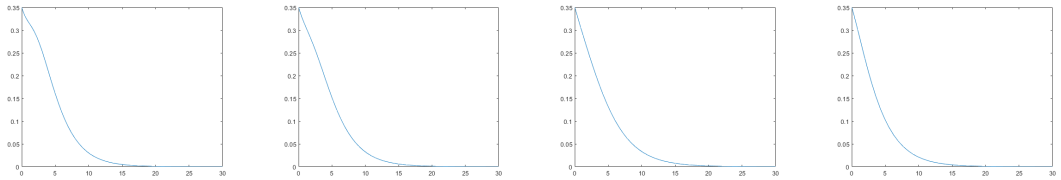

(a) (b) (c) (d)

Figure 3.10: Simulation of the original SIR model on the first node, with an initial conditions as $(x_1(0), y_1(0), z_1(0)) = (0.65, 0.35, 0)$ with the infection and recovery values respectively: $\beta = 0.55$ and $\gamma = 0.5$. The distance term ϵ is set, starting from the left, to $0, 0.2, 0.5, 1$.

As we expected, in the case of a decreasing trend since small ϵ values, this behaviour is emphasised as the interaction between the two parts weakens.

The conclusion that can be drawn from the above analysis is that the strengthening of the distance term ϵ within our model can not change the behaviour of the curve of the infected if they fall into one of the two standard cases provided by the scalar SIR, while it is able to mitigate or even eliminate the atypical behaviour. This consideration will be useful when we study different lockdown policies to be applied in order to contain the epidemic contagion.

3.1.4 Different infection rates

As an alternative interpretation, we can refer to the two nodes as separate age groups or different life-style populations in which not only a distance term, but also a differentiation of infection rates in the two nodes could be introduced. This concept is related to different susceptibility and vulnerability to the infectious disease. We can think that

some populations live in situations where there are more risky interactions, for example those who live in overcrowded urban apartments, use frequently public transportation, attends crowded places, etc. Let us begin by considering the differentiation in the rates of transmission of the epidemic. We can therefore discuss the following system in which the infection rate is no longer unique and constant as in the previous model.

$$\begin{cases} \dot{x}_i(t) = -\beta_i x_i(t) \sum_{j=1}^{n} a_{ij} y_j(t) \\ \dot{y}_i(t) = \beta_i x_i(t) \sum_{j=1}^{n} a_{ij} y_j(t) - \gamma y_i(t) \end{cases} \qquad i = 1,2 \tag{3.12}$$

where the graph weight matrix is defined with all entries equal to 1. In this model we assume that each node has its own way of reacting to the epidemic, expressed through its individual infection coefficient. Let us now analyse a series of simulations of this model, keeping the initial conditions constant in the two nodes and varying only the infection rate of the second node β_2.

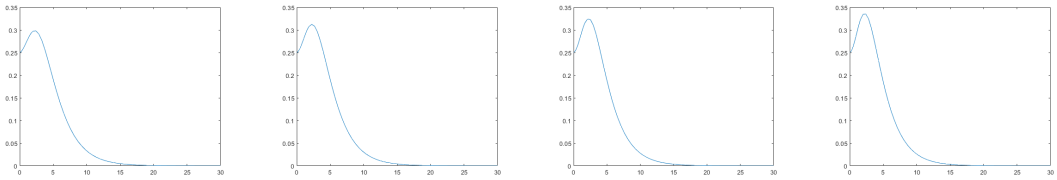

(a) (b) (c) (d)

Figure 3.11: Simulation of the original SIR model on the first node, with an initial conditions as $(x_1(0), y_1(0), z_1(0)) = (0.75, 0.25, 0)$ with the recovery rate $\gamma = 0.5$, the infection rate for the first node $\beta_1 = 0.7$, while for the second node, starting from the left, β_2 is set to $0.55, 0.65, 0.75, 0.85$.

The analysis above shows the behaviour of the curve as second node's infection rate changes, starting with cases where this rate is lower than the first node's one, assuming the second group most susceptible to infection. The general trend we can observe is definitely an increase in the peak of infection reached by the curve as β_2 increases, as was to be expected. Once again we see how the behaviour of the curve in the case of an epidemic outbreak is closely linked to conditions at the first node. Let us now analyse the behaviour of y_1, with another set of parameters.

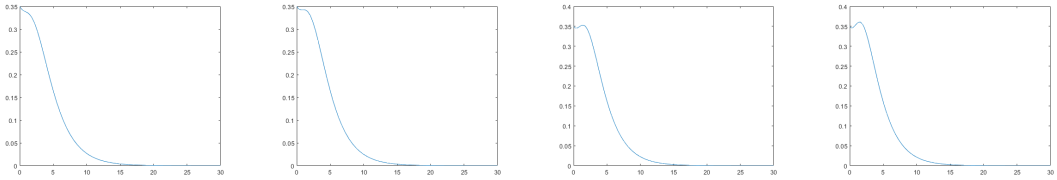

(a) (b) (c) (d)

Figure 3.12: Simulation of the original SIR model on the first node, with an initial conditions as $(x_1(0), y_1(0), z_1(0)) = (0.65, 0.35, 0)$ with the recovery rate $\gamma = 0.5$, the infection rate for the first node $\beta_1 = 0.65$, while for the second node, starting from the left, β_2 is set to $0.55, 0.65, 0.8, 0.9$.

As we can see above, increasing the infection rate in the second node leads to the formation of an infection peak in the first node's curve of infected, thus causing the occurrence of the atypical behaviour.

The next step at this point is the inclusion of the concept of distance between the two populations within the model considered at this stage. Let us therefore consider such a model where the graph adjacency matrix is differently defined, taking into account a possible distance term $\epsilon \in [0,1]$. There are several relevant cases that can be analysed at this stage, starting with the initial condition similar to the previous one where the infection is present in a single node. Considering this scenario, we can find the atypical phenomenon introduced earlier for certain values of the basic reproduction number, under different conditions from the one determined for the previous case with equal infection rates for the nodes.

Let us observe, for example, a series of simulations in which the infection rates are different at the two nodes, but with conditions at the first node similar to the simulations shown above in Figure 3.5, 3.6 and 3.7. Let us focus, at first, only on the dynamics of the infection concerning the first node.

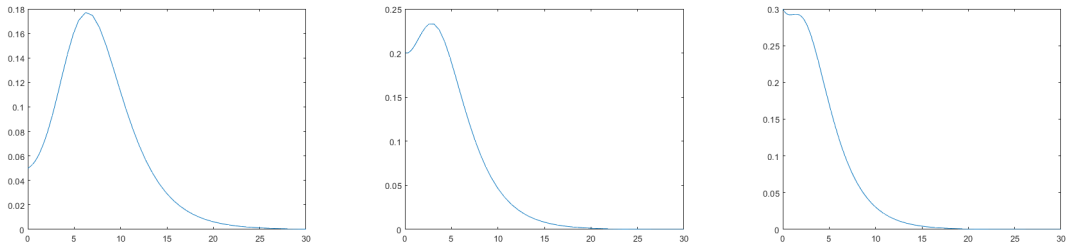

(a) (b) (c)

Figure 3.13: Simulation of the original SIR model on the first node, with the infection and recovery values respectively: $\beta_1 = 0.6$ and $\gamma = 0.5$, while the distance term ϵ is set to 0.2. The figure on the left is the curve of infected with an initial conditions as $(0.95, 0.05, 0)$ and $\beta_2 = 0.55$. In the middle, the simulation has initial conditions as $(0.8, 0.2, 0)$ and $\beta_2 = 0.65$. The figure on right hand has initial condition as $(0.7, 0.3, 0)$ and $\beta_2 = 0.8$.

As we can see, in the first case, the curve of the infected at the first node is such that it causes an epidemic outbreak despite β_2 being lower than β_1; in fact, this behaviour would occur whatever value is assigned to β_2, as long as the following is observed: $\beta_2/\gamma > 1$.
In the second figure, atypical behaviour is confirmed, with an increase in the second infection maximum compared to the case with equal infection rates, which is certainly due to the fact that we assumed a greater spread of the epidemic in the second node.
In the third case, however, the conditions at the first node are the same as previous simulation in Figure 3.7, but this time assuming a greater strength of the epidemic at the second node, as can be imagined in the case of a group that is more susceptible to infection and in which this virus spreads more. In the simulation with equal rates in the two nodes,

the condition on the first node led to decreasing behaviour, but now we can observe how the assumption that $\beta_2 \gg \beta_1$ leads to the occurrence of the non-classical behaviour.

Following this brief analysis, it is possible to state that the conditions on the first node, for which the atypical behaviour occurs, remain valid in this case but only if we consider a more diffuse infection in the second node. It is possible to consider also other combinations of the parameters that in the previous case would have led to a monotonous decrease, and instead with an increase of the β_2/β_1 ratio can lead to the atypical behaviour. This phenomenon can happen as it is sure that the model will start with $\dot{y_1}(0) < 0$, but β_2 is much greater than β_1, and it leads to a strong growth of the first derivative until it become positive. However, in the case of a strong weakening of the infection rate in the second node, it is possible that the atypical phenomenon, previously occurred, now no longer takes place; therefore the set of parameter values has changed compared to the previous case and the conditions obviously have to take into account the rate β_2.
On the other hand, the behaviour of the model in the second node is confirmed, i.e. an epidemic outbreak with a peak in infection and subsequent exponential decrease, whatever parameter values are used for the first node.

Another hyphotesis on infection rates A further interpretation of this interaction between two nodes within a graph may take into account that each infected individual has an infection rate linked to the node to which it belongs. The model generated following this assumption is as follows.

$$\begin{cases} \dot{x}_i(t) = -x_i(t) \sum_{j=1}^{n} \beta_j a_{ij} y_j(t) \\ \dot{y}_i(t) = x_i(t) \sum_{j=1}^{n} \beta_j a_{ij} y_j(t) - \gamma y_i(t) \end{cases} \qquad i = 1,2 \tag{3.13}$$

We compare several simulations of this version of the model using the same set of parameters, i.e. initial conditions for the nodes, infection and recover rates, that we considered for the previous model.

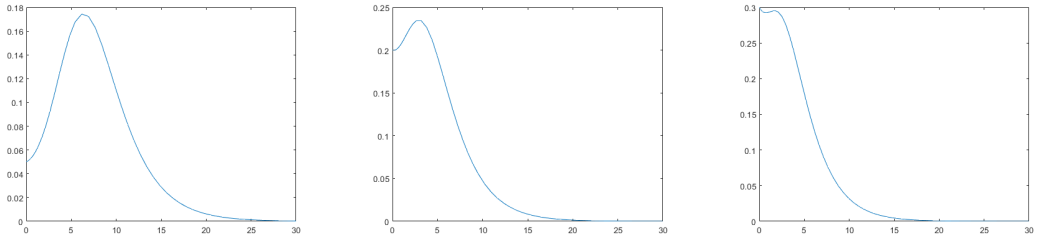

(a) (b) (c)

Figure 3.14: Simulation of the original SIR model on the first node. On the left figure (a), there is the infected curve with an initial conditions as $(0.8, 0.2, 0)$, infection and recovery values respectively as: $\beta_1 = 0.9$, $\beta_2 = 0.65$ and $\gamma = 0.5$, while the distance term ϵ is set to 0.2. In the middle (b), the simulation has same initial conditions and recover rate with $\beta_1 = 0.55$ and $\beta_2 = 0.7$, while ϵ is set to 0.1. The figure on right hand (c) has initial condition as $(0.75, 0.25, 0)$ with $\beta_1 = 0.55$, $\beta_2 = 0.95$. The distance term ϵ is set to 0.3.

From the figure above, we can see that the initial behaviour of the curve depends only on the conditions at the first node, so there is no difference from the previous simulation. As far as the second node is concerned, we always expect the same behaviour with unimodal dependence on time, with changes in the peak and the time at which it is reached depending on the parameters of epidemic and the distance term that were used.

In the following part, we will present simulations of the SIR model on simple networks initially, and then extend our analysis to more complex graphs, in which we will try to investigate the dynamic behaviour of the SIR model both in general on the network and in the each individual node, in order to observe the obtained results. We will then proceed with the introduction of mitigation measures of social interactions consequential to the propagation of the epidemic, as previously done for the scalar case.

3.2 SIR model on three nodes network

Let us now try to expand the discussion and see what happens in the case of a network consisting of three nodes in which the central node is the only one with an initial fraction of infected people. Let us assume that the central node is connected with the others with $\epsilon = 0$, and the model has the following initial conditions: $(x_i(0), y_i(0), z_i(0)) = (1, 0, 0)$ for $i = 1{,}3$ and $(x_2(0), y_2(0), z_2(0)) = (0.75, 0.25, 0)$, in which the second node has a percentage of infected as in the previous simulation but this time encounters two totally susceptible populations.

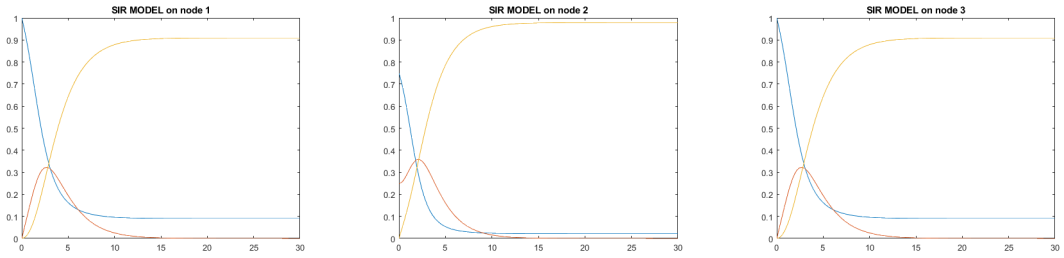

(a) (b) (c)

Figure 3.15: Simulation of the original SIR model on the three nodes network. The infection and recovery rates used have the following values respectively: $\beta = 0.7$ and $\gamma = 0.55$.

We can observe how in this case, despite the same initial condition, the infected curve of the second node shows a more marked behaviour than in the previous simulation with only two nodes. This example reinforces the idea of the *wave of return* suffered by the infected population because in this case the second node had been isolated it would not have seen the occurrence of the second epidemic peak. However, the encounter with two susceptible populations causes the new infected to infect the susceptibles of the second node leading to the advance of the curve to the maximum. The behaviour of the infected

curve in the other two nodes is the same, this is due to the fact that the graph is unweighted and the values of the infection and recover rates are the same for all three nodes, however the curve reaches a higher peak of infection than in the previous simulation.

Let us now suppose a smaller initial infection for this network, i.e. consider the initial conditions of the second node as $(x_2(0), y_2(0), z_2(0)) = (0.6, 0.4, 0)$ and observe the behaviour of the infected curve at the three nodes as done before.

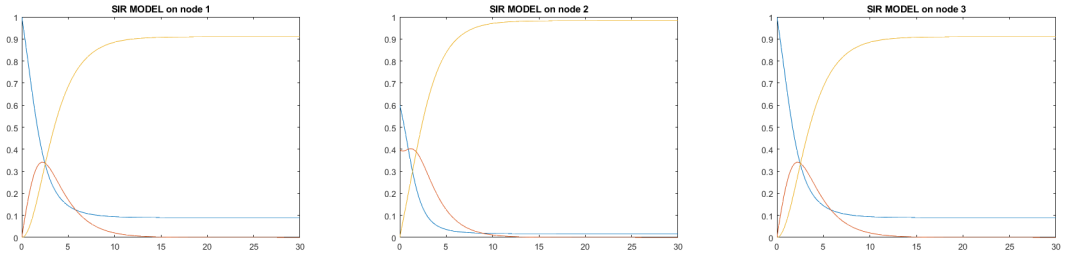

(a) (b) (c)

Figure 3.16: Simulation of the original SIR model on the three nodes network. The infection and recovery rates used have the following values respectively: $\beta = 0.7$ and $\gamma = 0.55$.

The behaviour of the nodes at the sides is the same as noted earlier, but as far as the central node is concerned, its initial reproduction number is equal to $R_{02} = 0.76$, and the behaviour of the curve is the atypical one. We can say that the increase in susceptible populations in contact with the infected one leads to a lowering of the threshold necessary for this behaviour to occur, with a fixed ϵ.

At this point, still within the study of the graph composed of three nodes, we also take a look at the case in which two nodes present an initial fraction of infected, for example we can suppose that the first node has initial condition as $(0.95, 0.05, 0)$, the third node as $(0.7, 0.3, 0)$, while the second is initially totally susceptible.

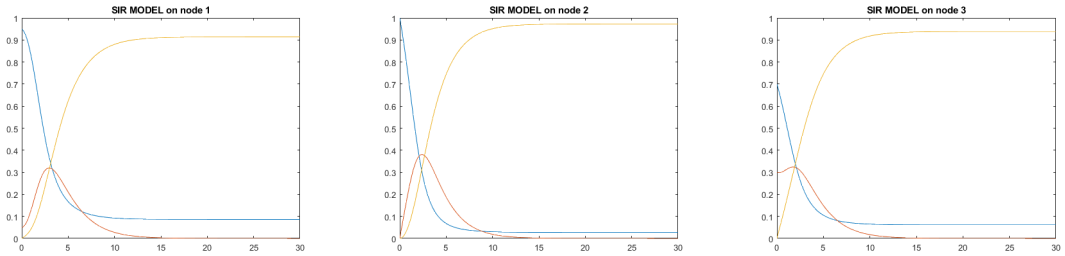

(a) (b) (c)

Figure 3.17: Simulation of the original SIR model on the three nodes network. The infection and recovery rates used have the following values respectively: $\beta = 0.6$ and $\gamma = 0.55$.

The behaviour on the first two nodes is classical, while on the third one we can see

that the non-classical phenomenon, we have already discussed, occurs again.

3.3 SIR model on star graph

Until now we have considered line type graphs, in which the propagation of the epidemic took place sequentially from the first infected node to the next. At this point we can observe what happens in the case of a star graph, i.e. one central node in communication with all the others, in which only the central one is infected, while the nodes outside are initially totally susceptibles. On the basis of what we have observed so far, we again expect to see the atypical behaviour of the infected curve of the central node, which undergoes the *return wave of infection* and presents an increasingly higher peak despite its initial conditions being such to cause a classical effective reproduction number below 1. Let us suppose a star graph composed by a central node with an initial amount of infected equal to $y(0) = 0.25$ and four external nodes totally susceptible.

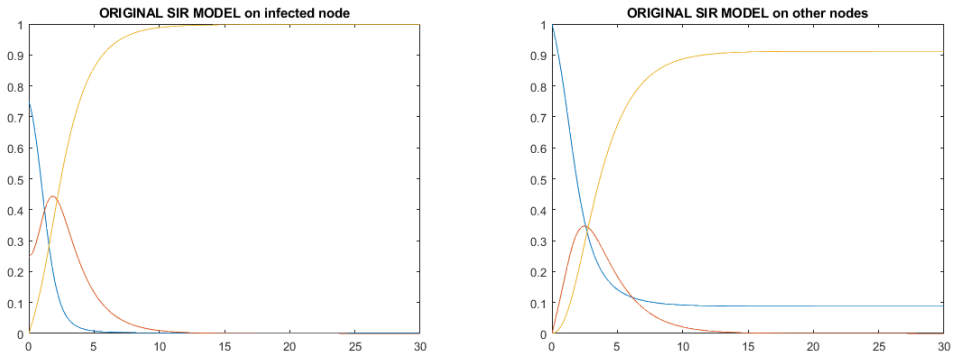

(a) (b)

Figure 3.18: Simulation of the original SIR model on the star graph with five nodes. On the left, there is the infected curve of the central node, while on the right there's the simulation on other nodes, being equal for all. The infection and recovery rates used have the following values respectively: $\beta = 0.7$ and $\gamma = 0.55$.

As mentioned above, the phenomenon is even more pronounced in this graph precisely because the central node undergoes a second infection from all the external nodes connected to it. In this case, the initial decrease in the curve seems to be almost attenuated and immediately starts with an increasing trend up to the peak and then decreases exponentially to 0. Compared to the cases of two or three nodes networks, here we can also see an increase in the peak and an advance in reaching it.

In the previous simulation we assumed that the central node was equally close to the leaf nodes, i.e. that the distance term ϵ was zero for the graph, whereas we now assume that the different nodes have a varying rate of closeness. Let us therefore assume that the four leaf nodes have the following distance terms: $0, 0.1, 0.2, 0.3$; as already observed in

the case of two nodes we expect it to cause a decrease in the infection peak, due precisely to the increase in the distance from the infected node.

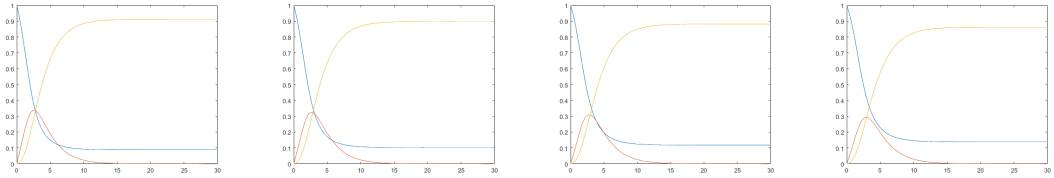

(a) (b) (c) (d)

Figure 3.19: Simulation of the original SIR model on the star graph with five nodes. The figures report only the simulation on the leaf nodes from the nearest to the furthest from the central one. The infection and recovery rates used have the following values respectively: $\beta = 0.7$ and $\gamma = 0.55$.

3.4 SIR model on line graph

Let us now consider a network consisting of a line of six nodes, where initially only the nodes at the extremes have a fraction of infected, while the central nodes are totally susceptible and let us observe the evolution of the infection on this graph.
We can assume the infection and recover rates as $\beta = 0.5$ and $\gamma = 0.4$ and as initial condition let's set then $(x(0), y(0), z(0) = (0.9, 0.1, 0)$ for the first node, $(1, 0, 0)$ for the central nodes and $(0.7, 0.3, 0)$ for the last one. In the following figure, we can find the simulation of the SIR model on the network described above.

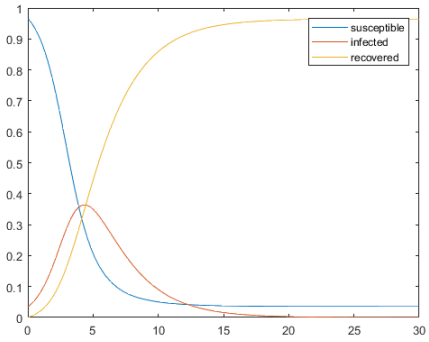

Figure 3.20: Simulation of the original SIR model on a network. The graph consists of six nodes where initially only the nodes at the extremes have a fraction of infected.

Considering the theorem mentioned in the initial part of this chapter, we are in the case of behaviour above the threshold and we can observe precisely the trend predicted by the theorem with regard to the average curve of the infected. In fact initially it grows

exponentially, reaches the peak of infection and then changes concavity and decreases to 0.

However, if we observe the progress of the infection in the individual nodes, we can observe a particular behavior regarding the sixth node.

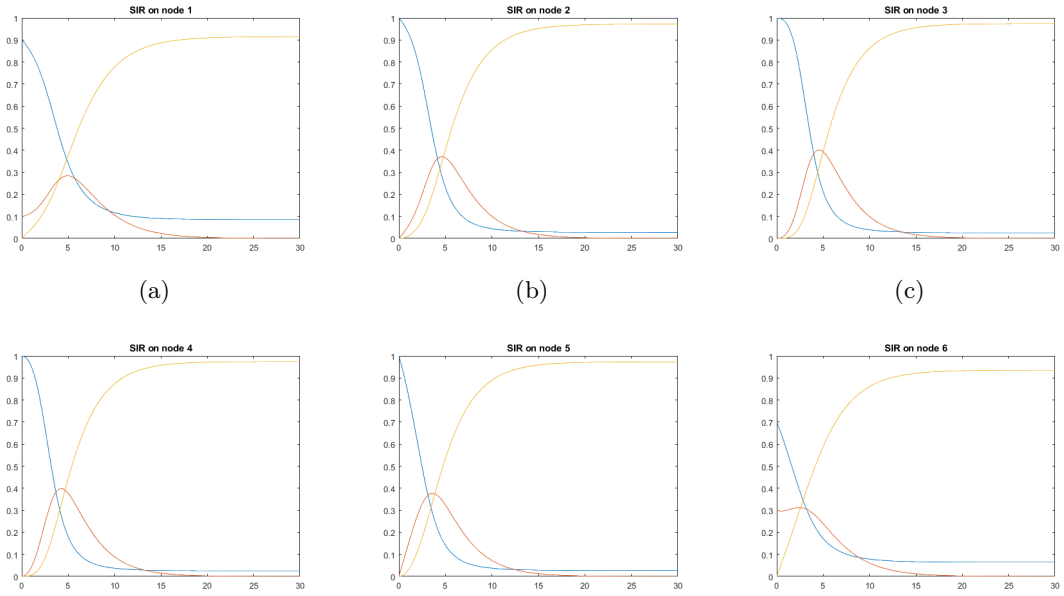

(a) (b) (c)

(d) (e) (f)

Figure 3.21: Simulation of the original SIR model on each node of the network composed of a line of six nodes.

As we can see, the trend in the previous nodes is consistent with what we expected based on the considerations made previously both on the scalar case and the network case, while the sixth node presents the atypical behavior demonstrated before. The initial reproduction number of the sixth node is $R_{06} = \beta x_6(0)/\gamma = 0.875 < 1$, therefore this initial value is such as not to cause an outbreak of the epidemic in the classical case; however we can notice that the infected curve initially decreases. After a few days we observe instead an increase up to the peak of infection, certainly caused by the wave of infection coming from the fixth node.

3.5 Modified Network SIR model

In this section we shall investigate several modified versions of the SIR-network model. As done previously, we consider a population split into a set of nodes, representing subpopulations that are different for geographical area or age. The interaction among these subpopulations is described through the weighted graph $\mathcal{G} = (\mathcal{V}, \mathcal{E}, A)$. We recall that $\mathcal{V}$ is the set of nodes, $\mathcal{E}$ is the links set that allow the spread of the infection and A is the weight

matrix and its entries a_{ij} embody the strength of the interaction between subpopulation i and subpopulation j. Therefore, we start from the SIR-network model

$$\begin{cases} \dot{x}_i(t) = -\beta x_i(t) \sum_{j=1}^{n} a_{ij} y_j(t) \\ \dot{y}_i(t) = \beta x_i(t) \sum_{j=1}^{n} a_{ij} y_j(t) - \gamma y_i(t) \\ \dot{z}_i(t) = \gamma y_i(t) \end{cases} \tag{3.14}$$

for all $i = 1, ..., n$. Let us remember that β is the infection rate, while γ is the recover rate. We decide to introduce a time variant social interaction mitigation term. We suppose this control function to be dependent on the vector of the infected fraction $y(t)$ in each node. This assumption is closely related to what we studied in Chapter 3 in the scalar case. In fact, the aim of this part is to integrate the concepts of population response to the epidemic and restrictive measures imposed by the government into the SIR-network model. In the various modified versions of the model, we assume a type of control with linear dependence on the number of infected. Unlike the analysis carried out on the scalar model in Chapter 2, here we are not interested in showing the different behaviour of the model on the basis of control policies with different dependency on the number of infected persons. In this case, the study will be aimed at investigating different lockdown strategies, assuming the same type of dependency on infected.

The main intervention hypotheses studied will be as follows: the application of control only in the interactions between different nodes, only within each individual node or in all interactions both inter-nodal and within the same subpopulation. The first type of control reflects an attempt to isolate different subpopulations by weakening the inter-nodal interaction so that in the case of the most infected node, the other nodes will not be too much affected. The second hypothesis involves a localised lockdown at each node, while contacts between different subpopulations are left unchanged. The last type of control is the most stringent, in which all types of interaction are restricted.

Suppose the application of these modified models in the network consisting of two nodes, where a distance term $\epsilon = 0.1$ is considered, so the weight matrix is

$$A = \begin{bmatrix} 1 & 0.9 \\ 0.9 & 1 \end{bmatrix}$$

Let us consider as initial conditions $(0.95, 0.05, 0)$ for the first node and $(0.7, 0.3, 0)$ for the second one and decide to set $\beta = 0.65$ and $\gamma = 0.5$. Below we can observe the simulation of the SIR-network without modifications on this graph.

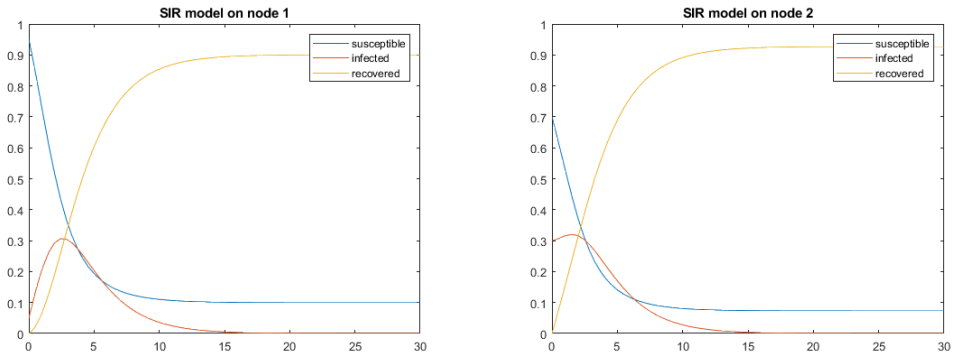

(a) (b)

Figure 3.22: Simulation of the classical SIR-network model on the two nodes with the infection and recovery values respectively: $\beta = 0.65$ and $\gamma = 0.5$. The distance term ϵ is set to 0.1.

We can now proceed with the explanation of the different ways of intervention and then observe the effect of these modifications on this network, with respect to the behaviour of the model without intervention, presented above.

3.5.1 Inter-nodal control

Let us start with the first hypothesis of epidemic control. We consider a term of mitigation of interactions only between individuals belonging to different nodes. If we consider nodes as geographically distinct subpopulations, this type of contact limitation will lead to a kind of distancing and isolation per area with movements restriction. The interpretation of nodes in this model as a subdivision of the population into age groups will instead result in a limitation of interactions between people of different ages. This may be justified by an attempt to avoid contact between stronger people and people in age groups more vulnerable to disease, for example. Let us remember that this function could be interpreted as a first intervention of governments control or an individual response of each node to the emergence of the epidemic. This reaction of the subpopulation is to close within itself and avoid external contacts. We will then consider the following model

$$\begin{cases} \dot{x}_i(t) = -\beta x_i(t) \left[a_{ii} y_i(t) + \sum_{j=1, j\neq i}^{n} a_{ij} y_j(t) f_{ij}(t) \right] \\ \dot{y}_i(t) = \beta x_i(t) \left[a_{ii} y_i(t) + \sum_{j=1, j\neq i}^{n} a_{ij} y_j(t) f_{ij}(t) \right] - \gamma y_i(t) \\ \dot{z}_i(t) = \gamma y_i(t) \end{cases} \tag{3.15}$$

where the term $f_{ij}(t)$ concerns the limitation of contacts between the individuals of population i and those population j. Obviously this term $f_{ij}(t)$ could depend on the infection level of both populations. In fact, with respect to what was explained before, the mitigation of contagion is attempted through lockdown functions linearly depending on the fraction of infected of the two populations involved in the contact.
For this reason, we can start by assuming that this term is equal to the product between

the individual lockdown terms within the populations, that is

$$f_{ij} = f_i f_j \quad \forall i, j = 1, ..., n$$

where the individual lockdown measures considered are the following functions

$$f_i(t) = 1 - y_i(t) \quad \forall i = 1, ..., n$$

We will therefore obtain that these terms introduced into the model are as follows

$$f_{ij} = f_{ji} = (1 - y_i(t))(1 - y_j(t)) \quad \forall i, j = 1, ..., n$$

We begin by considering the effect of this type of intervention in the network consisting of two nodes. We want to analyse the dynamical behaviour of this modified version into the previous presented network.

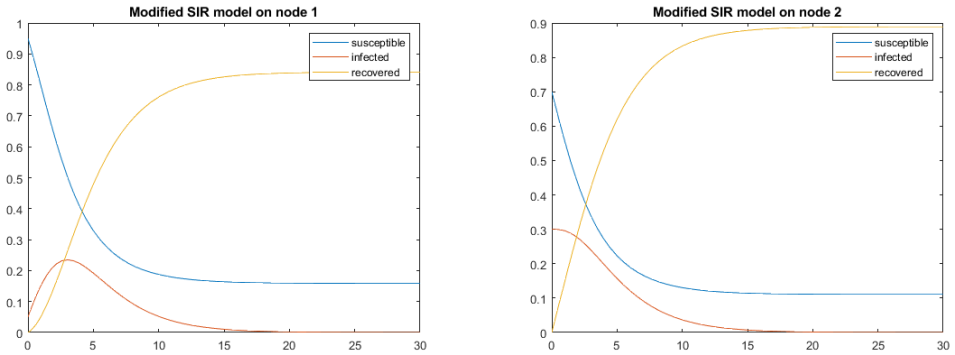

(a) (b)

Figure 3.23: Simulation of the first version of modified SIR model on the two nodes with the infection and recovery values respectively: $\beta = 0.65$ and $\gamma = 0.5$. The distance term ϵ is set to 0.1.

In the first case we see that the first node, whose classical effective reproduction number R_{01} is greater than 1, has an infected curve $y_1(t)$ that suffers a smoothing of the curve. The infection peak goes from about 0.3 reached after 2.4 days to about 0.23 reached on day 3. The second node has a greater fraction of initially infected than the first one, so with the same infection and recovery rates, it has a lower reproduction number, in fact $R_{02} < 1$. In the classical model, the curve of the infected in this node shows a unimodal behaviour, while with the imposed interventions, it changes to a monotonically decreasing trend. The interaction between the nodes in the classical model leads to an initially increasing trend of the second node, despite its R_{02} is less than 1. Therefore the encounter with the susceptibles of the first node causes the second infected curve $y_2(t)$ to assume an unimodal behaviour. On the other hand, in the modified SIR-network, the reduction of the interaction between the two nodes results in the disappearance of this phenomenon.

3.5.2 Localised control

The second hypothesis of intervention is opposite to the previous one. We assume that interactions are limited only within each subpopulation, while those between different nodes remain unchanged. This control policy might be the least realistic compared to the others. However, in our discussion, we are interested in analysing the behaviour of the SIR-network in the case of different interventions. We are not looking for an optimal or more easily applicable control, therefore let us just observe the effect of this modification. We analyse the following model

$$\begin{cases} \dot{x}_i(t) = -\beta x_i(t) \left[a_{ii} y_i(t) f_i^2(t) + \sum_{j=1, j\neq i}^{n} a_{ij} y_j(t) \right] \\ \dot{y}_i(t) = \beta x_i(t) \left[a_{ii} y_i(t) f_i^2(t) + \sum_{j=1, j\neq i}^{n} a_{ij} y_j(t) \right] - \gamma y_i(t) \\ \dot{z}_i(t) = \gamma y_i(t) \end{cases} \tag{3.16}$$

in which the intervention measures within the single node i are of the following type

$$f_i(t) = 1 - y_i(t) \quad \forall i = 1, ..., n$$

Let us now observe the behaviour of this modified model with a localised control in the network consisting of two nodes.

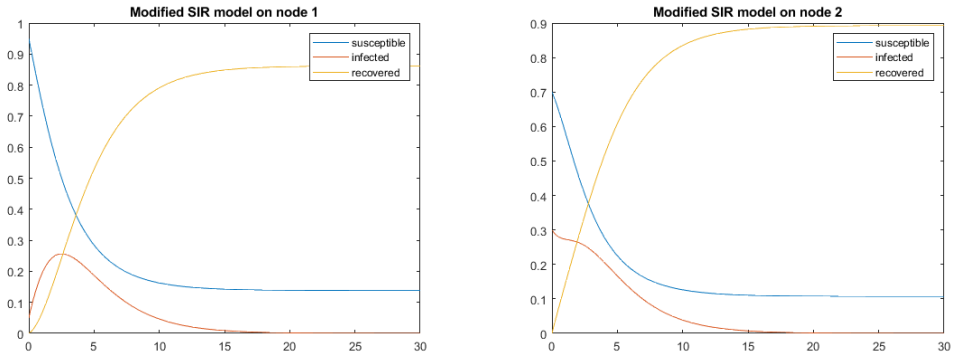

(a) (b)

Figure 3.24: Simulation of the second version of SIR-network model on the two nodes with the infection and recovery values respectively: $\beta = 0.65$ and $\gamma = 0.5$. The distance term ϵ is set to 0.1.

The intervention of the measures on the first node causes the peak to decrease to 0.26, while its time to reach it remains substantially unchanged. With regard to the second node, however, we observe a slightly different behaviour to that obtained in the previous simulation, although still decreasing. Also in this case, the limitation leads to the disappearance of the infection peak in the second node.

3.5.3 Total control

The most stringent control alternative is surely to combine the two previous hypotheses and apply a general lockdown. In this case we will therefore analyse the effect of inserting a contact mitigation term of any kind, i.e. both within each individual subpopulation and between different subpopulations. The considered modified SIR-network model will be

$$\begin{cases} \dot{x}_i(t) = -\beta x_i(t) \left[a_{ii} y_i(t) f_i^2(t) + \sum_{j=1, j\neq i}^{n} a_{ij} y_j(t) f_{ij}(t) \right] \\ \dot{y}_i(t) = \beta x_i(t) \left[a_{ii} y_i(t) f_i^2(t) + \sum_{j=1, j\neq i}^{n} a_{ij} y_j(t) f_{ij}(t) \right] - \gamma y_i(t) \\ \dot{z}_i(t) = \gamma y_i(t) \end{cases} \tag{3.17}$$

where the function $f_i(t)$ represents the term of lockdown concerning the social interactions between the individuals of the population i, while the term $f_{ij}(t)$ concerns the contacts between the individuals of different populations. As far as this last term is concerned, we always suppose it to be equal to the product between the single lockdown measures introduced in the populations that come into contact. In this case, the hypothesis acquires a greater meaning because it is natural to think that, in general, the greater the restrictions applied on the single population, the smaller will be the contacts between different populations. Noting that the third equation is redundant, with the previous hypothesis we can regard the system in the vector form as

$$\begin{cases} \dot{x}(t) = -\beta F(t) \left[diag(x(t))A \right] F(t) y(t) \\ \dot{y}(t) = \beta F(t) \left[diag(x(t))A \right] F(t) y(t) - \gamma y(t) \end{cases} \tag{3.18}$$

where F is a $n \times n$ diagonal matrix, whose inputs represent the individual social mitigation functions applied to the nodes that form the network in question. If we suppose $f_1(t)) = 1 - y_1(t)$, $\forall i$, then it results that $F(t) = diag(1 - y(t))$.
It is interesting to observe now the evolution of contagion in the both nodes of the network with these limitations.

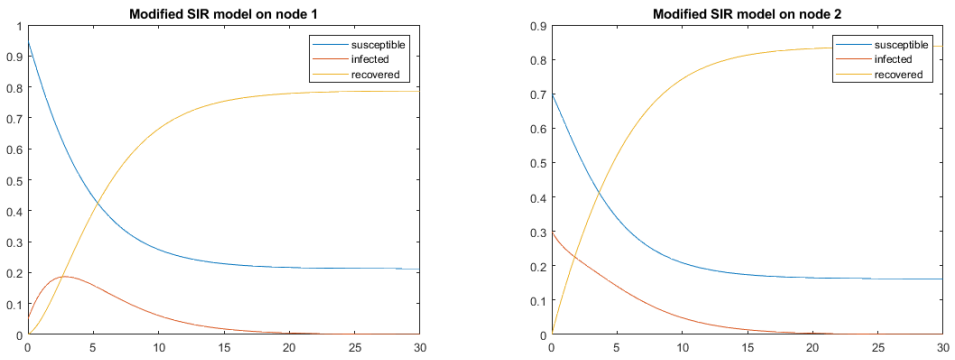

(a) (b)

Figure 3.25: Simulation of the third version of modified SIR-network model on the two nodes with the infection and recovery values respectively: $\beta = 0.65$ and $\gamma = 0.5$. The distance term ϵ is set to 0.1.

The curve of the infected in the first node undergoes a strong attenuation. Its infection peak goes from 0.3 (without control) to about 0.19, which is also lower than that obtained in the two previous cases. The final fraction of susceptibles increases considerably from 0.1 to 0.21, which is a direct consequence of the more restrictive measures applied to the population. In the second node we see an almost exponential decrease in the curve of the infected and, also in this case, an increase in the final fraction of susceptibles (from 0.07 to 0.16). In fact, we can conclude that the total control policy leads to a doubling of the final portion of susceptibles in both nodes compared to the unrestricted case.

Remaining in this hypothesis of "total" lockdown, i.e. a limitation of interactions between individuals not only belonging to different populations but also belonging to the same population, we try to use one of the functions studied previously for the scalar model. In fact, let us suppose that the individual lockdown measures are

$$f_i(t) = (1 - y_i^2(t))^\alpha \quad \forall i = 1, ..., n$$

with $\alpha > 0$. We look at the effect of this measure in the network under consideration. In the following simulations, we introduce in the model this type of limitation function with the exponent $\alpha = 7$.

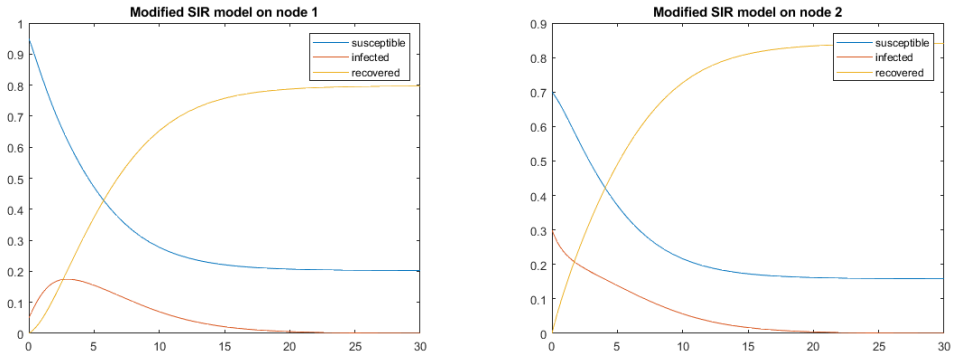

(a) (b)

Figure 3.26: Simulation of the fourth version of modified SIR-network model on the two nodes with the infection and recovery values respectively: $\beta = 0.65$ and $\gamma = 0.5$. The distance term ϵ is set to 0.1.

The behaviour at both nodes is almost identical to the previous case. We can only underline in the first node a stronger attenuation of the infected curve with a peak of about 0.17.

Chapter 4

Conclusion

In this thesis we examined the SIR compartmental model, the best known of the epidemiological models. The system of three coupled differential equations describes the evolution of a disease in a fully mixed closed population, encapsulating the mechanisms of contagion and spontaneous recovery. We studied the dynamical behaviour of the model both in scalar and network case with different infection scenarios.

Kermack and McKendrick's model is initially presented in the scalar case, where the importance of the parameter R_0 is emphasised from the outset. Depending on its value, two different epidemic behaviours are generated: initial exponential growth and subsequent decrease or monotonic decrease. Our main result, formalized in Theorem 2.1, concerns the behaviour of a generalised SIR model with a continuous control action, supposed dependent on the fraction of susceptible and infected individuals. Specifically, we defined a novel *effective reproduction number* as key element in determining the epidemics evolution. The considered mitigation term could be an expression of governments measures or a behavioural reaction of individuals after the occurrence of the epidemics. Through this function we have therefore modelled both a control action and an endogenous behaviour of the population. This modification affects the contact rate between individuals in the population and consequently also the rate of disease transmission.

We have considered a mitigation term that is only dependent on the infected and monotonically decreasing. We have analysed the behaviour of the model in the case of a linear, quadratic, smooth and smooth step control action. In this section, the aim was not to discuss optimal control in terms of smoothing the infection curve, but simply to compare models assuming different dependencies of control on the fraction of infected. We have observed, however, that the quadratic term leads to a higher final fraction of susceptibles than the other measures with the particular experimental set up we considered in the simulations. The question of whether to release the measurements after a certain time interval or not is then addressed. The concept of herd immunity level is introduced: it represents the level of the population immunity at which the spread of the disease will decline and stop even after the preventive measures have been relaxed. If this level is not reached during the intervention of the control, then a second wave of infection will occur once the action is eliminated. Considering a more realistic approach, a discontinuous control is analysed. Thinking of what is happening more recently in the fight against

the COVID-19 pandemic in Italy, we have considered a control activated only when the infection exceeds a predefined threshold level. Currently, the Italian regions are, in fact, divided into different risk bands on the basis of various factors, among which there is the number of confirmed infected cases, relative to the amount of diagnostic tests carried out. Therefore, the introduced model presents restrictive measures that are only activated above a certain level of infection. The long-term behaviour of the system within this strategy could consist of the so-called sliding motion, i.e. a very rapid transition between application and interruption of the control action. After an initial theoretical framework through Filippov's theory of discontinuous vector field systems, we examined two types of control: constant and non-constant. In the first case we defined conditions for the existence of the sliding mode in Proposition 2.36, while in the second case we limit ourselves to a specific analysis for a set of simulative data. We have seen that in both cases, discontinuous control can cause two different sliding mode behaviours. In the first case, the imposed threshold level is never exceeded by the number of infected, while in the second case an epidemic outbreak occurs even in the controlled system. A further adjustment to the classical SIR model concerns the consideration of a delay time between the observation of the epidemic and the subsequent individuals response or governments imposed measures, in order to obtain a better description. The combination of the concept of discontinuous control and time delay leads to a new model that we have analysed. We can observe a continuous transition between the unrestrictive and the restrictive model. In contrast to sliding mode, there is no perfect slipping on the surface separating the two systems, but rather a continuous crossing from one model to the other, the so-called chattering phenomenon. As we said, our analysis was not focused on finding optimal control, but this could be a future development. We could then deepen the study of the model by searching for the best control (always intended as mitigation of social interactions dependent on the fraction of infected) that is able to minimise the cost of lives and the economic cost, considering limited available resources. Another improvement would be to diversify the control action and the individuals self-regulation models, studying a coupled system of epidemis and evolutionary game dynamics.

In Chapter 3, the SIR model has been investigated in the network case. We presented a result, shown in [5], that provides a new threshold condition for the average behaviour of the system. The average considered was weighted by the eigenvector of a particular matrix. Above this condition, expressed in terms of network characteristics, initial conditions and infection parameters, the epidemic initially grows, while below it dies. We then turn to the case of a network consisting of only two nodes. Initially we derived the Corollary 3.1.1 that explicits the conditions of the theorem mentioned earlier in the particular two nodes case. Within the study of this graph, we analysed the behaviour of the model at each node as well and highlighted an atypical phenomenon compared to the results of the theory on classical SIR. This phenomenon consists of the appearance of two peaks of infection and occurs when a subpopulation with a fraction of infected encounters a second totally susceptible subpopulation. The specific scenario causes a return wave of infection and leads the initially infected node to have a second peak, where the first one is its initial condition. We then conducted analyses on the behaviour of the infected curve of the first node as the initial conditions and the distance term between the two nodes changed. We noted that increasing the distance between the nodes can certainly make the second

infection peak disappear if it occurred for closer nodes, but neither of the two behaviours outlined by the classical theory can be changed. A differentiation between infection rates in the two nodes is introduced and the simulations conducted confirm what said above. On the other hand, simulations of the model with unique infection rate are carried out on other types of network. In the final Section 3.5, we introduced a control action in the SIR network model. Specifically, we presented three systems with different lockdown hyphothesis: firstly, a control applied only in the interactions between nodes; then only within each individual node and finally, in all interactions both internodal and within the same subpopulation. This last part could certainly be expanded and better investigated. A future goal could be a theorisation of the results on the modified SIR network, e.g. a parallel result to Theorem 3.1 on the average behaviour of the model with control. The discussion could then consider different lockdown policies for each node and study their effect.

References

[1] URL: https://covid19.who.int/.

[2] Kermack William Ogilvy and McKendrick Anderson G. "A contribution to the mathematical theory of epidemics". In: *Proceedings of the Royal Society of London. Series A* (1927), pp. 700–721.

[3] Hethcote Herbert W. "The mathematics of infectious disease". In: *SIAM Review* 42.4 (2000), pp. 599–653.

[4] Newman M. E. J. "Spread of epidemic disease on networks". In: *Physical Review E* 66.1 (2002).

[5] Mei Wenjun et al. "On the dynamics of deterministic epidemic propagation over networks". In: *Annual Reviews in Control* 44 (2017), pp. 116–128.

[6] Alvarez Fernando E., Argente David, and Lippi Francesco. "A simple planning problem for Covid-19 lockdown". In: *National Bureau of Economic Research* w26981 (2020).

[7] Acemoglu Daron et al. "Optimal targeted lockdowns in a multi-group SIR model". In: *National Bureau of Economic Research* w27102 (2020).

[8] Hansen Elsa and Day Troy. "Optimal control of epidemics with limited resources". In: *Journal of Math. Biology* 62.3 (2011), pp. 423–451.

[9] Birge John R., Candogan Ozan, and Feng Yiding. "Controlling Epidemic Spread: Reducing Economic Losses with Targeted Closures". In: 57 (2020).

[10] Funk Sebastian et al. "The spread of awareness and its impact on epidemic outbreaks". In: *Prot. of the National Academy of Sciences* 106.16 (2009).

[11] Verelst Frederik, Willem Lander, and Beutels Philippe. "Behavioural change models for infectious disease transmission: a systematic review (2010– 2015)". In: *J. R. Soc. Interface*. 13th ser. 125.20160820 (2016).

[12] Xiao Yanni, Xu Xiaxia, and Tang Sanyi. "Sliding Mode Control of Outbreaks of Emerging Infectious Diseases". In: *Bulletin of Mathematical Biology* (2012), pp. 2403–2422.

[13] URL: https://en.wikipedia.org/wiki/Sliding_mode_control.

[14] Filippov A. F. *Differential Equations with Discontinuous Righthand Sides. Control System*. Mathematics and Its Applications. Ed. by Arscott F.M. 1988.

[15] Dieci Luca and Lopez Luciano. "On Filippov and Utkin Sliding Solution of Discontinuous Systems". In: *9th SIMAI Conference - Applied and Industrial Mathematics in Italy II* (2009).